

Event-Driven Receding Horizon Control For Distributed Persistent Monitoring on Graphs

Shirantha Welikala and Christos G. Cassandras

Abstract—We consider the optimal multi-agent persistent monitoring problem defined on a set of nodes (targets) interconnected through a fixed graph topology. The objective is to minimize a measure of mean overall node state uncertainty evaluated over a finite time interval by controlling the motion of a team of agents. Prior work has addressed this problem through on-line parametric controllers and gradient-based methods often leading to low-performing local optima or through off-line computationally intensive centralized approaches. This paper proposes a computationally efficient event-driven receding horizon control approach providing a distributed on-line solution to the persistent monitoring problem. A novel element in the controller is that it self-optimizes the planning horizon over which control actions are sequentially taken in event-driven fashion. Numerical results show significant improvements compared to state of the art distributed on-line parametric control solutions.

I. INTRODUCTION

A *persistent monitoring* problem arises when a dynamically changing environment is monitored by a set of mobile agents and encompasses applications such as environmental sensing [1], surveillance systems [2], energy management [3] and data collection [4]. In contrast to cases where every point in the environment is equally valued for agents to monitor, in many others, only a finite set of “points of interest” (henceforth called “targets”) holds a positive value [5], [6]. The persistent monitoring problem considered in this paper belongs to the latter class, where the goal of the agent team is to monitor (sense or collect information from) each target in order to reduce an “uncertainty metric” associated with the target state. Typically, this uncertainty metric increases when no agent is monitoring (sensing) the target and decreases when one or more agents are able to monitor it by dwelling in its vicinity. The global objective is to control the agent movement so as to minimize an overall measure of target uncertainties.

Persistent monitoring problems in 1D environments have been solved using classical optimal control techniques. For such problems, the optimal solutions have been shown to be threshold-based parametric controllers [7]. However, this synergy between optimal control and parametric controllers does not extend to 2D environments [8]. Nevertheless, one can still optimize agent trajectories within parametric families [8], [9] (e.g., elliptical). Apart from the apparent sub-optimality, failing to react to dynamic changes in target

uncertainties and the dependence of performance on the initial target/agent conditions are drawbacks of this approach. As a solution, recent work [5] has proposed a graph abstraction (where targets are modeled as nodes and inter-target agent trajectory segments are modeled as edges) to formulate *Persistent Monitoring on Graphs* (PMG) problems.

In PMG problems, an agent trajectory is defined by the sequence of *targets to be visited* and the *dwell time* spent at each visited target. To overcome the complexity of this problem, a *distributed* Threshold-based Control Policy (TCP) is adopted in [5], where each agent enforces a set of thresholds on its neighboring target uncertainty values to make immediate trajectory decisions: the dwell time to be spent and the next target to visit. The threshold values are then optimized using an *on-line* gradient-based technique based on Infinitesimal Perturbation Analysis (IPA) [10]. However, this IPA-TCP approach often converges to poor locally optimal solutions. As a remedy, [6] has proposed to append an *off-line centralized* threshold initialization scheme which is shown to considerably increase performance at the expense of significant computational effort. Moreover, since on-line control is still governed by the IPA-TCP method, any state perturbation would trigger a new parameter tuning process with a considerable amount of recovery time.

Motivated by these challenges, this paper presents an entirely different approach that can be used to solve the same PMG problem. Specifically, the event-driven nature of PMG systems is exploited to derive an Event-Driven Receding Horizon Controller (ED-RHC) to optimally govern each of the agents in an on-line distributed manner using only a minimal amount of computational power. First, it is shown that each agent’s trajectory is fully characterized by the sequence of decisions it makes at specific discrete event times. Second, for any agent, a *Receding Horizon Control Problem* (RHCP) is formulated to determine locally optimal decisions over a planning horizon, to be executed only over a shorter action horizon with the process sequentially repeated as new events take place. In contrast to earlier uses of this approach [11], [12], [13] the proposed ED-RHC includes the ability to simultaneously determine the optimal value of the planning horizon to be used. Next, a number of structural properties of this RHCP (a non-convex constrained optimization problem) are exploited to derive solutions in closed form.

The paper is organized as follows. Section II presents the problem formulation, some preliminary results and an overview of the ED-RHC solution. Sections III, IV and V presents how the ED-RHC problem is explicitly solved. Fi-

*Supported in part by NSF under grants ECCS-1509084, DMS-1664644, CNS-1645681, by AFOSR under grant FA9550-19-1-0158, by ARPA-E’s NEXTCAR program under grant DE-AR0000796 and by the MathWorks.

The authors are with the Division of Systems Engineering and Center for Information and Systems Engineering, Boston University, Brookline, MA 02446, {shiran27, cgc}@bu.edu.

nally, the proposed ED-RHC method is implemented and its performance is compared with the IPA-TCP solution through simulation results in Section VI. Section VII concludes the paper.

II. PROBLEM FORMULATION

A. Persistent Monitoring On Graphs (PMG) Problem

Consider an n -dimensional mission space containing M targets (nodes) in the set $\mathcal{T} = \{1, 2, \dots, M\}$ where the location of target i is fixed at $Y_i \in \mathbb{R}^n$. A team of N agents in the set $\mathcal{A} = \{1, 2, \dots, N\}$ is deployed to monitor the targets. Each agent $a \in \mathcal{A}$ moves within this space and its location at time t is denoted by $s_a(t) \in \mathbb{R}^n$.

a) **Target Model:** Each target $i \in \mathcal{T}$ has an associated uncertainty state $R_i(t) \in \mathbb{R}$ which follows the dynamics:

$$\dot{R}_i(t) = \begin{cases} A_i - B_i N_i(t) & \text{if } R_i(t) > 0 \text{ or } A_i - B_i N_i(t) > 0 \\ 0 & \text{otherwise,} \end{cases} \quad (1)$$

where $N_i(t) = \sum_{a \in \mathcal{A}} \mathbf{1}\{s_a(t) = Y_i\}$ ($\mathbf{1}\{\cdot\}$ is the indicator function) and the values of $A_i, B_i, R_i(0)$ are prespecified. Therefore, $N_i(t)$ is the number of agents present at target i at time t . According to (1): (i) $R_i(t)$ increases at a rate A_i when no agent is visiting target i , (ii) $R_i(t)$ decreases at a rate $B_i N_i(t) - A_i$ where B_i is the uncertainty removal rate by a visiting agent (i.e., agent sensing or data collection rate) to the target i , and, (iii) $R_i(t) \geq 0, \forall t$. This problem set-up has an attractive queueing system interpretation [5] where A_i and $B_i N_i(t)$ are respectively thought of as the arrival rate and the controllable service rate at target (server) $i \in \mathcal{T}$ in a queueing network.

b) **Agent Model:** Some persistent monitoring models (e.g., [7], [14]) assume each agent $a \in \mathcal{A}$ to have a finite sensing range $r_a > 0$ allowing it to decrease $R_i(t)$ whenever it is in the vicinity of target $i \in \mathcal{T}$ (i.e., when $\|s_a(t) - Y_i\| \leq r_a$). Since we will adopt a graph topology for this problem, the condition $\|s_a(t) - Y_i\| \leq r_a$ is represented by the agent residing at the i th vertex of a graph and $N_i(t)$ is used to replace the role of the joint detection probability of a target i used in [7], [14]. Moreover, similar to [6] the analysis in this paper is independent of the agent motion dynamic model.

c) **Objective:** Our objective is to minimize the mean system uncertainty J_T over a finite time interval $t \in [0, T]$:

$$J_T \triangleq \frac{1}{T} \int_0^T \sum_{i \in \mathcal{T}} R_i(t) dt, \quad (2)$$

by controlling the motion of the agents through a suitable set of feasible controls to be described in the sequel.

d) **Graph Topology:** A directed graph topology $\mathcal{G} = (\mathcal{T}, \mathcal{E})$ is embedded into the mission space such that the targets are represented by the graph vertices $\mathcal{T} = \{1, 2, \dots, M\}$, and the inter-target trajectory segments are represented by the graph edges $\mathcal{E} \subseteq \{(i, j) : i, j \in \mathcal{T}\}$. We point out that these trajectory segments in \mathbb{R}^n may take arbitrary shapes so as to account for potential constraints in the agent motion; in the graph \mathcal{G} , each segment represented by an edge $(i, j) \in \mathcal{E}$ has an associated value $\rho_{ij} \in \mathbb{R}_{\geq 0}$

representing the *transit time* an agent spends to travel from target i to j . The *neighbor set* and the *neighborhood* of a target $i \in \mathcal{T}$ are defined respectively as

$$\mathcal{N}_i \triangleq \{j : (i, j) \in \mathcal{E}\} \text{ and } \bar{\mathcal{N}}_i = \mathcal{N}_i \cup \{i\}. \quad (3)$$

e) **Control:** Based on this embedded graph topology \mathcal{G} , whenever an agent $a \in \mathcal{A}$ is ready to leave a target $i \in \mathcal{T}$, it selects a *next-visit* target $j \in \mathcal{N}_i$. Hence, the agent travels over $(i, j) \in \mathcal{E}$ to arrive at target j after an amount of time ρ_{ij} . Subsequently, it selects a *dwell-time* $\tau_j \in \mathbb{R}_{\geq 0}$ to spend at target j (which contributes to decreasing $R_j(t)$), and then makes another next-visit decision.

Therefore, in a PMG problem the control exerted consists of a sequence of *next-visit* targets $j \in \mathcal{N}_i$ and *dwell-times* $\tau_i \in \mathbb{R}_{\geq 0}$. Our goal is to determine (τ_i, j) for any agent residing at i at any time $t \in [0, T]$ which are optimal in the sense of minimizing (2). As pointed out in [5], this is a challenging task even for the simplest PMG problem configurations due to the nature of the search space.

f) **Receding Horizon Control:** The on-line distributed IPA-TCP method proposed in [5] requires each agent to use a set of *thresholds* applied to its neighborhood target uncertainties $\{R_j(t) : j \in \mathcal{N}_i\}$ in order to determine its dwell-time and next-visit decisions. Thus, the objective in (2) is viewed as dependent on these threshold parameters. Starting from an arbitrary set of thresholds, each agent iteratively adjusts them using a gradient technique that exploits the information from observed events in agents' trajectories. Although this approach is efficient due to the use of IPA, it is limited by the presence of local optima.

To address this limitation, this paper proposes an *Event-Driven Receding Horizon Controller* (ED-RHC) at each agent $i \in \mathcal{T}$. The basic idea of RHC has its root in Model Predictive Control (MPC) but, in addition, it exploits the event-driven nature of the PMG problem to reduce complexity by orders of magnitude, provide flexibility in the frequency of control updates, and improve performance by avoiding many local optima resulting from gradient-based optimization. As introduced in [11] and extended in [12],[13], ED-RHC solves an optimization problem of the form (2) but limited to a given *planning horizon* whenever an event is observed; the resulting control is then executed over a generally shorter *action horizon* defined by the occurrence of the next event of interest to the controller. This process is iteratively repeated in event-driven fashion. In the PMG problem, the aim of the ED-RHC when invoked at time t with an agent residing at $i \in \mathcal{T}$ is to determine the immediate next-visit $j \in \mathcal{N}_i$ and dwell times at i, j , jointly forming a control $U_i(t)$. This is done by solving an optimization problem of the form:

$$U_i^*(t) = \arg \min_{U_i(t) \in \mathbb{U}(t)} [J_H(X_i(t), U_i(t); H) + \hat{J}_H(X_i(t+H))], \quad (4)$$

where $X_i(t)$ is the current local state and $\mathbb{U}(t)$ is the feasible control set at t . The term $J_H(X_i(t), U_i(t); H)$ is the immediate cost over the planning horizon $[t, t+H]$ and $\hat{J}_H(X_i(t+H))$ is an estimate of the future cost evaluated at the end of

the planning horizon $t + H$. The value of H is selected in prior work [11],[12],[13] *exogenously*. However, in this paper we will include this value into the optimization problem and ignore the $\hat{J}_H(X_i(t+H))$ term. Thus, by optimizing the planning horizon we compensate for the complexity and intrinsic inaccuracy of $\hat{J}_H(X_i(t+H))$. Moreover, note that the proposed ED-RHC is *distributed* since it allows each agent to separately solve (4) using only local state information.

B. Preliminary Results

According to (1), the target state $R_i(t)$, $i \in \mathcal{T}$, is piece-wise linear and its gradient $\dot{R}_i(t)$ changes only when one of the following (strictly local) *events* occurs: (i) An agent arrival at i , (ii) $[R_i(t) \rightarrow 0^+]$, or (iii) An agent departure from i . Let the occurrence of such events be indexed by $k = 1, 2, \dots$ with an associated occurrence time t_i^k with $t_i^0 = 0$. Then,

$$\dot{R}_i(t) = \dot{R}_i(t_i^k), \quad \forall t \in [t_i^k, t_i^{k+1}). \quad (5)$$

Remark 1: If a control constraint is imposed so that agents dwell on target i in a *non-overlapping* manner (i.e., one agent at a time), then $N_i(t) \in \{0, 1\}$, $\forall t \in [0, T]$ in (1) and it follows from (5) that the sequence $\{\dot{R}_i(t_i^k)\}$, $k = 0, 1, 2, \dots$, is a *cyclic order* of three elements: $\{-(B_i - A_i), 0, A_i\}$. As pointed out in [6], allowing overlapping dwell sessions at some target (also known as “target sharing”) is known to lead to poor performance (clearly, this concern does not apply to single-agent problems). This observation motivates the next assumption.

Assumption 1: The controller is constrained to enforce the non-overlapping condition $N_i(t) \in \{0, 1\}$, $\forall t \in [0, T]$, $i \in \mathcal{T}$.

To make sure that each agent is capable of enforcing the event $[R_i \rightarrow 0^+]$ at any $i \in \mathcal{T}$, the following simple stability condition is assumed (similar to [6]).

Assumption 2: Target uncertainty rate parameters A_i and B_i of each target $i \in \mathcal{T}$ satisfy $0 < A_i < B_i$.

a) Decomposition of the objective function: The following Theorem 1 provides a target-wise and temporal decomposition of the main objective function J_T in (2).

Theorem 1: The contribution to the main objective J_T by a target $i \in \mathcal{T}$ during a time period $[t_0, t_1] \subseteq [t_i^k, t_i^{k+1})$ for some $k \in \mathbb{Z}_{\geq 0}$ is $\frac{1}{T} J_i(t_0, t_1)$, where,

$$J_i(t_0, t_1) = \int_{t_0}^{t_1} R_i(t) dt = \frac{(t_1 - t_0)}{2} [2R_i(t_0) + \dot{R}_i(t_0)(t_1 - t_0)]. \quad (6)$$

Proof: In (2), by taking the summation operator out of the integration and then splitting the time interval $t \in [0, T]$ of the integration of $R_i(t)$ profile into three parts gives

$$J_T = \frac{1}{T} \left[\sum_{j \in \mathcal{T} \setminus \{i\}} \int_0^T R_j(t) dt \right] + \frac{1}{T} \left[\int_0^{t_0} R_i(t) dt + \int_{t_0}^{t_1} R_i(t) dt + \int_{t_1}^T R_i(t) dt \right], \quad (7)$$

where $\cdot \setminus \cdot$ represents the set subtraction operator. Therefore, clearly the contribution of target i to the main objective J_T

during the time period $t \in [t_0, t_1]$ is $\frac{1}{T} J_i(t_0, t_1)$ where,

$$J_i(t_0, t_1) = \int_{t_0}^{t_1} R_i(t) dt.$$

Moreover, since $[t_0, t_1] \subseteq [t_i^k, t_i^{k+1})$, the relationship (5) implies that $\int_{t_0}^{t_1} R_i(t) dt$ represents the area of a trapezoid (whose parallel sides are $R_i(t_0)$ and $R_i(t_1)$). Therefore,

$$J_i(t_0, t_1) = \left[\frac{R_i(t_0) + R_i(t_1)}{2} \times (t_1 - t_0) \right].$$

Also, (5) gives that $R_i(t_1) = R_i(t_0) + \dot{R}_i(t_0)(t_1 - t_0)$. Therefore,

$$J_i(t_0, t_1) = \frac{(t_1 - t_0)}{2} [2R_i(t_0) + \dot{R}_i(t_0)(t_1 - t_0)]. \quad \blacksquare$$

A simple corollary of Theorem 1 is to extend it to any interval $[t_0, t_1]$ which may include one or more event times t_i^k . In particular:

Corollary 1: Let $t_i^k = t_0$ be the time when an agent arrives at target $i \in \mathcal{T}$ and let the next two events be strictly local to target i : (i) $[R_i(t_i^{k+1}) \rightarrow 0^+]$ and (ii) agent departure at $t = t_i^{k+2}$. For any t_1 is such that $t_i^{k+2} \leq t_1 < t_i^{k+3}$,

$$J_i(t_0, t_1) = \frac{u_i}{2} [2R_i(t_0) - (B_i - A_i)u_i] + \frac{r_i}{2} [A_i r_i],$$

where $u_i = t_i^{k+1} - t_0$ and $r_i = t_1 - t_i^{k+2}$.

Proof: Applying Theorem 1 to the three interested inter-event intervals gives

$$J_i(t_0, t_1) = \frac{(t_i^{k+1} - t_0)}{2} [2R_i(t_0) + \dot{R}_i(t_0)(t_i^{k+1} - t_0)] + \frac{(t_i^{k+2} - t_i^{k+1})}{2} [2R_i(t_i^{k+1}) + \dot{R}_i(t_i^{k+1})(t_i^{k+2} - t_i^{k+1})] + \frac{(t_1 - t_i^{k+2})}{2} [2R_i(t_i^{k+2}) + \dot{R}_i(t_i^{k+2})(t_1 - t_i^{k+2})].$$

Now, using: (i) the definitions of u_i, r_i , (ii) the \dot{R}_i values stated in Remark 1 and (iii) the fact that $R_i(t_i^{k+1}) = R_i(t_i^{k+2}) = 0$, the above expression can be simplified as

$$J_i(t_0, t_1) = \frac{u_i}{2} [2R_i(t_0) - (B_i - A_i)u_i] + \frac{v_i}{2} [2 * 0 + 0 * v_i] + \frac{r_i}{2} [2 * 0 + A_i r_i], \\ = \frac{u_i}{2} [2R_i(t_0) - (B_i - A_i)u_i] + \frac{r_i}{2} [A_i r_i]. \quad \blacksquare$$

b) Local objective function: In the distributed setting we have established, *local* information is shared by neighboring targets. In particular:

- 1) Target $i \in \mathcal{T}$ receives the information $\{A_j, B_j\}$ at $t = 0$ from its neighbors $j \in \mathcal{N}_i$.
- 2) Target $i \in \mathcal{T}$ receives information $\{R_j(t), \dot{R}_j(t)\}$ at any time t from its neighbors $j \in \mathcal{N}_i$.
- 3) Any agent $a \in \mathcal{A}$ residing at target $i \in \mathcal{T}$ at time t (i.e., $s_a(t) = Y_i$) can obtain the above two types of information from any neighboring target $j \in \mathcal{N}_i$.

The *local objective function* of target i over a time period $[t_0, t_1) \subseteq [0, T]$ is defined as

$$\bar{J}_i(t_0, t_1) = \sum_{j \in \mathcal{N}_i} J_j(t_0, t_1). \quad (8)$$

The value of each $J_j(t_0, t_1)$ above is obtained through Theorem 1 and its extension Corollary 1 if $[t_0, t_1)$ includes additional events: $[t_0, t_1)$ is decomposed into a sequence of corresponding inter-event time intervals.

C. ED-RHC optimization problem formulation

Let agent $a \in \mathcal{A}$ reside at target $i \in \mathcal{T}$ at some $t \in [0, T]$. In our distributed setting, we assume that agent a is made aware of only *local events* occurring in the neighborhood \mathcal{N}_i . As mentioned earlier, the control $U_i(t)$ consists of the *dwelt time* τ_i at the current target i , and the *next target* $j \in \mathcal{N}_i$ to visit. Once j is known, then the agent can also determine the *dwelt time* τ_j at the next target j . Moreover, a dwelt time decision τ_i (or τ_j) can be divided into two interdependent decisions: (i) the *active time* u_i (or u_j) and (ii) the *inactive* (or *idle*) time v_i (or v_j), as shown in Fig. 1. Thus, agent a has to optimally choose five *decision variables* which form the control vector $U_i(t) = [u_i(t), v_i(t), j, u_j(t), v_j(t)]$.

a) Fixed Planning Horizon: Recalling (4), the ED-RHC depends on the planning horizon $H \in \mathbb{R}_{\geq 0}$ which is viewed as a *fixed* control parameter. Note that $t + H$ is constrained by $t + H \leq T$, hence if this is violated we redefine the planning horizon to be $H = T - t$. For simplicity, in what follows we omit this situation which only arises as the process approaches the terminal time T .

Let us decompose the control $U_i(t)$ into its real-valued components and its discrete (target index $j \in \mathcal{N}_i$) component. Thus (omitting time arguments), set $U_{ij} = [u_i, v_i, u_j, v_j]$ and let the current local state be $X_i(t) = \{R_j(t) : j \in \mathcal{N}_i\}$. Then, the optimal controls are obtained by solving the following set of optimization problems, henceforth called the ED-RHC Problem (RHCP):

$$U_{ij}^* = \arg \min_{U_{ij} \in \mathbb{U}} J_H(X_i(t), U_{ij}; H); \quad \forall j \in \mathcal{N}_i, \text{ and}, \quad (9)$$

$$j^* = \arg \min_{j \in \mathcal{N}_i} J_H(X_i(t), U_{ij}^*; H). \quad (10)$$

Note that (9) involves solving a number $|\mathcal{N}_i|$ of optimization problems, one for each $j \in \mathcal{N}_i$. Then, (10) determines j^* through a simple numerical comparison. Therefore, the final optimal decision variables are $U_{ij^*}^*$ and j^* . Here, the notation $|\cdot|$ denotes the 1-norm or the cardinality operator when the argument is respectively a vector or a set.

The objective function $J_H(\cdot)$ above is chosen to reflect the contribution to the main objective J_T in (2) by the targets in

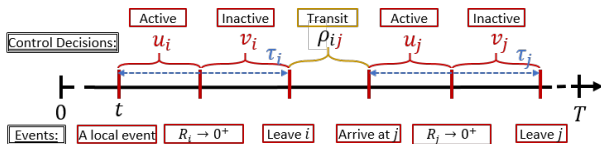


Fig. 1: Event timeline and control decisions under RHC.

the neighborhood \mathcal{N}_i over the time period $[t, t + H]$, which is provided by (8) and Theorem 1 as

$$J_H(X_i(t), U_{ij}; H) = \frac{1}{H} \bar{J}_i(t, t + H), \text{ and}, \\ \mathbb{U} = \{U : U \in \mathbb{R}^4, U \geq 0, |U| + \rho_{ij} = H\}. \quad (11)$$

The *feasible control space* \mathbb{U} in (9) is such that u_i, v_i, u_j, v_j are non-negative real variables. In addition, note that since $|U_{ij}| + \rho_{ij} = H$ (see also Fig.1) this restricts the choices of the four control variables. Thus, the selection of H affects the problem's optimal solution. For example, if H is very large (or very small), clearly the optimal decisions U_{ij}^* and j^* are not globally optimal. Attempting to find the optimal choice of H without compromising the on-line distributed nature of the ED-RHC solution is a challenging task.

b) Variable Planning Horizon: To address this problem, we introduce a *variable horizon* w as:

$$w \triangleq |U_{ij}| + \rho_{ij} = u_i + v_i + \rho_{ij} + u_j + v_j, \quad (12)$$

and replace H in (11) by w while, at the same time, imposing the constraint: $w \leq H$. Therefore, the objective function J_H and the feasible control space \mathbb{U} in the RHCP are chosen as

$$J_H(X_i(t), U_{ij}; H) = \frac{1}{w} \bar{J}_i(t, t + w), \text{ and}, \\ \mathbb{U} = \{U : U \in \mathbb{R}^4, U \geq 0, |U| + \rho_{ij} \leq H\}. \quad (13)$$

Note that, the constraint $|U_{ij}| + \rho_{ij} \leq H$ above ensures $w \leq H$. Moreover, this novel RHCP formulation allows us to simultaneously determine the *optimal planning horizon* size $w^* = |U_{ij^*}^*| + \rho_{ij^*}$ in terms of the optimal control $U_i^*(t)$.

On the other hand, having a control-dependent denominator term in the objective function and adding an extra dimension to the feasible control space of the RHCP introduce new technical challenges that we address in the rest of the paper. To accomplish this, we will exploit structural properties of (13) and show that the RHCP in (9) can be solved analytically and efficiently.

c) Event-Driven Action Horizon: As in all RHCPs, the solution of each optimization problem over a planning horizon H is executed only over an *action horizon* $h \leq H$. In the ED-RHC setting, the value of h is determined by the first event that takes place after t (when the RHCP was last solved). Thus, in contrast to time-driven RHC, the control is updated whenever asynchronous events occur; this prevents unnecessary steps to re-solve the RHCP (9)-(10) with (13).

Figure 2 shows an example of three consecutive action horizons (labeled h_1, h_2 and h_3) observed by an agent a after an event at t triggers the solution of the RHCP with a planning horizon H . Note that w_1, w_2, w_3 represent the three optimal control-dependent horizon sizes (i.e., $w^*(U_i^*)$ values) determined at each respective local event time: $t, t + h_1$ and $t + h_1 + h_2$.

In general, the determination of the action horizon h may be controllable or uncontrollable. The latter case occurs as a result of random events in the system (if such events are part of the setting), while the former corresponds to

the occurrence of any one event whose occurrence results from an agent solving a RHCP. We define next the three *controllable* events associated with an agent when it resides at target i ; each of these events defines the action horizon h following the solution of a RHCP by this agent at some time $t \in [0, T]$:

2. Event $[h \rightarrow v_i^*]$: This event occurs at time $t + v_i^*(t)$. It is only feasible after an event $[h \rightarrow u_i^*]$ has occurred, including the possibility that $u_i^*(t) = 0$ in the RHCP solution determined at t . Clearly, this coincides with a departure event from target i .

Observe that these events are mutually exclusive, i.e., only one is feasible at any one time. It is also possible for a different event to occur after t and before one of these occurs; such an event is either random (if our model allows for such events) or it is controllable but associated with a different target than i . In particular, let us define two additional events that may occur at any neighbor $j \in \mathcal{N}_i$ and affect the agent residing at i . These events are a consequence of Assumption 1 and pertain only to multi-agent persistent monitoring problems, where our controller must enforce the no-target-sharing policy.

we set

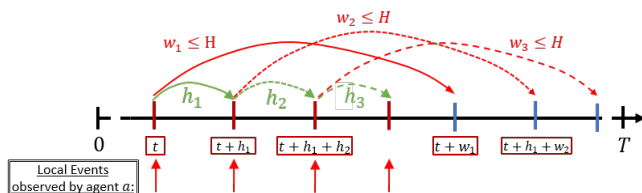
The effect of this modification is clear if a RHCP solved by an agent at target i at some time t leads to a next visit solution $j^* \in \mathcal{N}_i$, and if this is followed by an event at $t' > t$ causing j^* to be covered, then $\mathcal{N}_i(t') = \mathcal{N}_i(t) \setminus \{j^*\}$ and the agent at i (whether active or inactive) must re-solve the RHCP at t' with the new $\mathcal{N}_i(t')$. Note that as soon as an agent a is en route to j^* , then j^* becomes covered, hence preventing any other agent from visiting j^* prior to agent a 's subsequent departure from j^* .

4. Covering Event C_j , $j \in \mathcal{N}_i$: This event causes $\mathcal{N}_i(t)$ to be modified to $\mathcal{N}_i(t) \setminus \{j\}$.

If one of these two events takes place while an agent residing at target i is either active or inactive, then the RHCP (9)-(10) is re-solved to account for the updated $\mathcal{N}_i(t)$. This may affect the values of the optimal solution U_i^* from the previous solution. Note, however, that the new solution will still give rise to an event $[h \rightarrow u_i^*]$ (if the RHCP is solved while the agent is active) or $[h \rightarrow v_i^*]$ (if the RHCP is solved while the agent is inactive).

RHCP1: This problem is solved by an agent when an event $[h \rightarrow \rho_{ki}]$ occurs at time t for any $k \in \mathcal{N}_i(t)$, i.e., the agent arrives at target i . The solution $U_i^*(t)$ includes $u_i^*(t) \geq 0$, representing the amount of time that the agent should be active at i . This problem may also be solved while the agent is active at i if a C_j or \bar{C}_j event occurs for any $j \in \mathcal{N}_i(t)$.

RHCP3: This problem is solved by an agent residing at i when an event $[h \rightarrow u_i^*]$ occurs at time t and $R_i(t) > 0$. The solution $U_i^*(t)$ is again constrained to include $u_i^*(t) = 0$ by default; in addition, it is constrained to have $v_i^*(t) = 0$ since the agent ceases being active while $R_i(t) > 0$, implying that it must immediately depart from i without becoming inactive. This problem is also solved when an event $[h \rightarrow v_i^*]$ occurs at time t , implying that the agent departs from i .



neighbor $m \in \mathcal{N}_i \setminus \{j\}$ during the future time period $[t, t+w)$ (see (13), (8) and Theorem 1).

However, this task becomes tractable when the aforementioned neighbor-set modification in (14) is employed. For example, upon using (14), if some neighbor $m \in \mathcal{N}_i(t)$, then, there is no other agent residing in or en route to target m at t . Therefore, clearly, $\dot{R}_m(\tau) = A_m$ for the period $\tau \in [t, t+r)$ where $r \geq \min_{q \in \mathcal{N}_m} \rho_{qm}$. Now, if $[t, t+r) \subseteq [t, t+w)$, projections are used to estimate the remaining portion of the $R_m(\tau)$ profile (i.e. for $\tau \in [t+r, t+w)$). This enables expressing $\bar{J}_i(t, t+w)$ analytically.

f) **Complexity of RHCPs:** As we will show next, all three problem forms of the RHCP can be solved in closed form. Therefore, their complexity is constant and the overall RHC complexity scales linearly with the number of events in $[0, T]$.

III. SOLVING THE EVENT-DRIVEN RECEDING HORIZON CONTROL PROBLEM FORM - 3 (RHCP3)

As discussed before, an agent has to evaluate **RHCP3** when it is ready to leave its residing target. Therefore, **RHCP3** involves only three decision variables: j and $U_{ij} \triangleq [u_j, v_j]$ (as $u_i^* = 0$ and $v_i^* = 0$ by default in this case). Out of these three decision variables, the obtained optimum choice for $j = j^*$ is directly taken as the next destination to visit (i.e., the "Action"). Therefore, **RHCP3** plays a crucial role in defining each agent's trajectory.

As shown in Fig. 1 (with $u_i = 0$ and $v_i = 0$), upon leaving target i at time t , the agent a plans to visit neighbor target j and spend an active time of u_j and an inactive time of v_j on j . The variable horizon (i.e., w in (12)) for this case is $w = |U_{ij}| + \rho_{ij} = \rho_{ij} + u_j + v_j$. According to the feasible control space definition in (13), w should be constrained so that $\rho_{ij} \leq w \leq H$ where H is the known fixed planning horizon. Therefore, targets $j \in \mathcal{N}_i$ where $\rho_{ij} > H$ are omitted from evaluating (9). Thus, $\rho_{ij} \leq H$ is assumed henceforth in this section.

a) **Constraints:** As mentioned in Section II-C, the decision variables u_j and v_j are inter-dependent due to the nature of the target uncertainty dynamics (1). Specifically, any dynamically feasible decision pair (u_j, v_j) should belong to one of the two classes defined below:

$$\begin{cases} \text{Class 1: } 0 \leq u_j \leq u_j^B \text{ and } v_j = 0, \text{ or,} \\ \text{Class 2: } u_j = u_j^B \text{ and } v_j \geq 0 \end{cases} \quad (15)$$

where u_j^B is the maximum active time possible to spend on target j - which will make $R_j \rightarrow 0$ under the given initial conditions. Using (1), u_j^B can be written as

$$u_j^B = \frac{R_j(t) + \rho_{ij}}{B_j - A_j} = \frac{R_j(t) + A_j \rho_{ij}}{B_j - A_j}. \quad (16)$$

Note that u_j^B is a constant that only depends on: initial target uncertainty $R_j(t)$, target parameters A_j, B_j , and transit time ρ_{ij} . Moreover, note the fact that in order to spend a non zero inactive time (i.e., $v_j > 0$), the agent has to first spend the maximum active time possible (i.e., $u_j = u_j^B$). Also, note that the decision: $(u_j^B, 0)$ is common to both classes.

Now, the above two classes are redefined to incorporate the horizon constraint: $w = |U_{ij}| + \rho_{ij} \leq H$ as follows.

$$\begin{cases} \text{Class 1: } 0 \leq u_j \leq \bar{u}_j \text{ and } v_j = 0, \text{ or,} \\ \text{Class 2: } u_j = u_j^B \text{ and } 0 \leq v_j \leq \bar{v}_j, \end{cases} \quad (17)$$

where u_j^B is given in (16) and

$$\begin{aligned} \bar{u}_j &\triangleq \min\{u_j^B, H - \rho_{ij}\}, \text{ and,} \\ \bar{v}_j &\triangleq H - (\rho_{ij} + u_j^B). \end{aligned}$$

Here, \bar{u}_j and \bar{v}_j represent the maximum possible u_j and v_j values respectively. Now, any control decision $U_{ij} = [u_j, v_j]$ that follows (17) is feasible for the **RHCP3**, i.e., $U_{ij} \in \mathbb{U}$ in (13).

b) **Objective:** According to the generic RHCP objective function definition given in (13), the objective function corresponding to the **RHCP3** is taken as $J_H(U_{ij})$ where

$$J_H(U_{ij}) = J_H(X_i(t), [0, 0, U_{ij}]; H) = \frac{1}{w} \bar{J}_i(t, t+w).$$

To obtain an expression for J_H , first, the local objective function \bar{J}_i is decomposed as (using (8))

$$\bar{J}_i = J_j + \sum_{m \in \mathcal{N}_i \setminus \{j\}} J_m. \quad (18)$$

Now, considering the state trajectories (as shown in Fig. 3) for the case where agent a goes from target i to target j following decisions u_j and v_j , both J_j and J_m terms in (18) are evaluated for the period $[t, t+w)$ using Theorem 1. This gives

$$\begin{aligned} J_j &= \frac{\rho_{ij}}{T} [2R_j(t) + A_j \rho_{ij}] + \frac{u_j}{T} [2(R_j(t) + A_j \rho_{ij}) \\ &\quad - (B_j - A_j)u_j], \text{ and} \\ J_m &= \frac{(\rho_{ij} + u_j + v_j)}{T} [2R_m(t) + A_m(\rho_{ij} + u_j + v_j)]. \end{aligned}$$

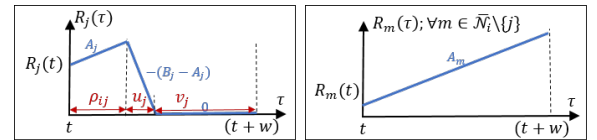


Fig. 3: State trajectories during $[t, t+w)$ for the **RHCP3**

Now, combining the above two results and substituting it in (18) gives the complete objective function $J_H(U_{ij})$ as

$$J_H(u_j, v_j) = \frac{C_1 u_j^2 + C_2 v_j^2 + C_3 u_j v_j + C_4 u_j + C_5 v_j + C_6}{\rho_{ij} + u_j + v_j}, \quad (19)$$

where,

$$\begin{aligned} C_1 &= \frac{1}{2} [\bar{A} - B_j], \quad C_2 = \frac{\bar{A}_j}{2}, \quad C_3 = \bar{A}_j, \quad C_4 = [\bar{R}(t) + \bar{A} \rho_{ij}], \\ C_5 &= [\bar{R}_j(t) + \bar{A}_j \rho_{ij}], \quad C_6 = \frac{\rho_{ij}}{2} [2\bar{R}(t) + \bar{A} \rho_{ij}], \end{aligned}$$

and (the neighborhood parameters)

$$\begin{aligned}\bar{A}_{ij} &= \sum_{m \in \mathcal{N}_i \setminus \{j\}} A_m, \quad \bar{R}_{ij}(t) = \sum_{m \in \mathcal{N}_i \setminus \{j\}} R_m(t), \\ \bar{A}_i &= \bar{A}_{ij} + A_j, \quad \bar{A}_j = \bar{A}_{ij} + A_i, \quad \bar{A} = \bar{A}_{ij} + A_i + A_j, \\ \bar{R}_i &= \bar{R}_{ij} + R_j, \quad \bar{R}_j = \bar{R}_{ij} + R_i, \quad \bar{R} = \bar{R}_{ij} + R_i + R_j.\end{aligned}\quad (20)$$

Note that all the coefficients stated above are non-negative except for C_1 which is non-negative only when: $B_j \leq \bar{A}$.

c) **Solving the RHCP3 for optimal control** (u_j^*, v_j^*):

Based on the first step of RHCP (9), (u_j^*, v_j^*) is given by

$$\begin{aligned}(u_j^*, v_j^*) &= \arg \min_{(u_j, v_j)} J_H(u_j, v_j) \\ (u_j, v_j) &\text{ s.t. (17).}\end{aligned}\quad (21)$$

- **Class 1:** First, assume (u_j^*, v_j^*) belongs to the Class 1 defined in (17). Then, $v_j = v_j^* = 0$ and (21) takes the form:

$$\begin{aligned}u_j^* &= \arg \min_{u_j} J_H(u_j, 0) \\ 0 &\leq u_j \leq \bar{u}_j.\end{aligned}\quad (22)$$

where \bar{u}_j is given in (17).

Lemma 1: The optimal solution for (22) is

$$u_j^* = \begin{cases} \bar{u}_j & \text{if } \bar{u}_j \geq u_j^\# \text{ and } \bar{A} < B_j, \\ 0 & \text{otherwise,} \end{cases}\quad (23)$$

where

$$u_j^\# = \frac{\bar{A}\rho_{ij}}{B_j - \bar{A}}.\quad (24)$$

Proof: Using (19), first and second order derivatives of $J_H(u_j, 0)$ can be obtained respectively as $J'(u_j)$ and $J''(u_j)$, where

$$\begin{aligned}J'(u_j) &= \frac{\bar{A} - B_j}{2} + \frac{B_j \rho_{ij}^2}{2(\rho_{ij} + u_j)^2}, \text{ and} \\ J''(u_j) &= -\frac{B_j \rho_{ij}^2}{(\rho_{ij} + u_j)^3}.\end{aligned}$$

Notice that $J'(0) > 0$ and $J''(u_j) < 0, \forall u_j \geq 0$. This implies that $J'(u_j)$ is monotonically decreasing with $u_j \geq 0$. Also note that $\lim_{u_j \rightarrow \infty} J'(u_j) = \frac{\bar{A} - B_j}{2}$.

Therefore, for the case where $\bar{A} \geq B_j$, the objective $J_H(u_j, 0)$ is monotonically increasing with u_j . Hence $u_j^* = 0$ in (22).

For the case where $\bar{A} < B_j$, the limiting value of $J'(u_j)$ is negative. This implies an existence of a maximum (of $J_H(u_j, 0)$) at some $u_j \geq 0$. However, such a maximizing u_j value is irrelevant to (22). Nevertheless, a crucial u_j value is located at the point where $J_H(0, 0) = J_H(u_j, 0)$ occurs. Using (19), this can be determined as $u_j = \frac{C_6 - C_4 \rho_{ij}}{C_1}$ which simplifies to $u_j = u_j^\#$ where $u_j^\#$ is given in (24).

According to the nature of $J'(u_j)$ and $J''(u_j)$, it is clear that $J_H(u_j, 0)$ should be decreasing with $u_j \geq u_j^\#$ (below $J_H(0, 0)$ value). Therefore, when $\bar{u}_j \geq u_j^\#$ (and $\bar{A} < B_j$), $u_j^* = \bar{u}_j$ in (22). ■

Note that $u_j^\#$ in (24) can be thought of as a break-even point for u_j , where when \bar{u}_j allows u_j to go beyond such a $u_j^\#$ value, it is always optimal to do so by choosing $u_j = \bar{u}_j$.

Remark 2: When H is sufficiently large, according to (17) and (16), $\bar{u}_j = u_j^B = \frac{R_j(t) + A_j \rho_{ij}}{B_j - A_j}$. Therefore, the condition $\bar{u}_j \geq u_j^\#$ used in (22) becomes state dependent (specifically on $R_j(t)$). For a such case, u_j^* in (22) becomes

$$u_j^* = \begin{cases} \bar{u}_j & \text{if } R_j(t) \geq \rho_{ij} \left[\frac{B_j - A_j}{B_j - \bar{A}} \cdot \bar{A} - A_j \right] \text{ and } \bar{A} < B_j \\ 0 & \text{otherwise.} \end{cases}\quad (25)$$

- **Class 2:** Now, assume (u_j^*, v_j^*) belongs to the Class 2 defined in (17). Then, $u_j = u_j^* = u_j^B$ and (21) takes the form:

$$\begin{aligned}v_j^* &= \arg \min_{v_j} J_H(u_j^B, v_j) \\ 0 &\leq v_j \leq \bar{v}_j.\end{aligned}\quad (26)$$

Lemma 2: The optimal solution for (26) is

$$v_j^* = \begin{cases} 0 & \text{if } \bar{A} \geq B_j \left[1 - \frac{\rho_{ij}^2}{(\rho_{ij} + u_j^B)^2} \right] \\ v_j^\# & \text{else if } v_j^\# \leq \bar{v}_j \\ \bar{v}_j & \text{otherwise,} \end{cases}\quad (27)$$

where

$$v_j^\# = \sqrt{\frac{(B_j - A_j)(\rho_{ij} + u_j^B)^2 - B_j \rho_{ij}^2}{\bar{A}_j}} - (\rho_{ij} + u_j^B).\quad (28)$$

Proof: Similar to the proof of Lemma 1, using (19), first and second order derivatives of $J_H(u_j^B, v_j)$ with respect to v_j can be obtained respectively as $J'(v_j)$ and $J''(v_j)$, where

$$\begin{aligned}J'(0) &= \frac{\bar{A}}{2} - \frac{B_j}{2} \left[1 - \frac{\rho_{ij}^2}{(\rho_{ij} + u_j^B)^2} \right], \text{ and} \\ J''(v_j) &= \frac{R_j^2(t) + 2B_j \rho_{ij} R_j(t) + A_j B_j \rho_{ij}^2}{(B_j - A_j)(\rho_{ij} + u_j^B + v_j)}.\end{aligned}$$

Note that $J''(v_j) > 0$ for all $v_j \geq 0$. This implies that $J_H(u_j^B, v_j)$ is convex in the positive orthant of v_j , and $J'(v_j)$ is increasing with $v_j \geq 0$ starting from $J'(0)$ given above.

Now, if $J'(0) \geq 0$, it implies that $J_H(u_j^B, v_j)$ is monotonically increasing with $v_j \geq 0$. Therefore, for such a case, $v_j^* = 0$ and it proves the first case in (27).

When $J'(0) < 0$, there should exist a minimum to $J_H(u_j^B, v_j)$ at some $v_j \geq 0$. Using calculus, the minimizing v_j value can be found easily as $v_j = v_j^\#$ given in (28).

Now, based on the constraint $0 \leq v_j \leq \bar{v}_j$ in (27) and the convexity of $J_H(u_j^B, v_j)$, it is clear that whenever $v_j^\# \leq \bar{v}_j \implies v_j^* = v_j^\#$ in (27) and whenever $v_j^\# > \bar{v}_j \implies v_j^* = \bar{v}_j$. This proves the last two cases given in (27). ■

Unlike $u_j^\#$ given in (24) for the problem (22), $v_j^\#$ given in (28) for the problem (26) is an optimal choice available for v_j . Therefore, whenever the constraints on v_j (i.e., $0 \leq v_j \leq \bar{v}_j$) allow choosing $v_j = v_j^\#$, it should be executed.

Remark 3: The terms u_j^B and \bar{v}_j involved in (27) can be simplified (using (16) and (17) respectively) to illustrate the

state dependent nature of v_j^* as

$$v_j^* = \begin{cases} 0 & \text{if } \bar{A} \geq B_j \text{ or } R_j(t) \leq \left[\frac{\rho_{ij}(B_j - A_j)\sqrt{B_j}}{\sqrt{B_j - \bar{A}}} - \rho_{ij}B_j \right] \\ v_j^\# & \text{else if } R_j(t) \leq \left[\sqrt{(B_j - A_j)(H^2\bar{A} + \rho_{ij}^2B_j)} - \rho_{ij}B_j \right] \\ \bar{v}_j & \text{otherwise.} \end{cases} \quad (29)$$

- **Combined Result:**

Theorem 2: The optimal solution of (21) is

$$(u_j^*, v_j^*) = \begin{cases} (0, 0) & \text{if } u_j^\# > \bar{u}_j \text{ or } \bar{A} \geq B_j \\ (\bar{u}_j, 0) & \text{else if } \bar{u}_j < u_j^\# \\ (u_j^\#, 0) & \text{else if } B_j > \bar{A} \geq B_j \left[1 - \frac{\rho_{ij}^2}{(\rho_{ij} + u_j^\#)^2} \right] \\ (u_j^\#, v_j^\#) & \text{else if } v_j^\# \leq \bar{v}_j \\ (u_j^\#, \bar{v}_j) & \text{otherwise,} \end{cases} \quad (30)$$

where $u_j^\#$ is given in (24) and $v_j^\#$ is given in (28).

Proof: This result is a composition of the respective solutions given in Lemma 1 and 2 for the optimization problems (22) and (26). ■

Based on the cases where the first condition in (30) is not satisfied, the following remark can be made.

Remark 4: The above theorem implies that whenever: (i) the fixed time horizon H is sufficiently large, (ii) the sensing capabilities are higher $B_j > \bar{A}$ and (iii) target uncertainty $R_j(t)$ is larger than some known threshold, it is optimum to plan ahead to empty the target j 's uncertainty upon visiting it (i.e., $u_j^* = u_j^\#$). This conclusion is inline with the Theorem 1 proposed in [5].

d) Solving for optimum next destination j^ :* Using Theorem 2, when the agent a is ready to leave target i at some local event time t , it can compute the optimal trajectory costs $J_H(u_j^*, v_j^*)$ for all $j \in \mathcal{N}_i$. Note that $J_H(u_j^*, v_j^*)$ is heavily dependent on $\{R_j(t), \bar{u}_j, \bar{v}_j, A_j, B_j, \rho_{ij}\}$ values.

Having such a dependence is crucial. Appendix B provides a counter example where the same **RHCP3** have been considered but with a different objective function form (other than (13)). For that case, it is proven that (see Theorem 4 and (69)) $J_H(u_j^*, v_j^*)$ is dependent only on ρ_{ij} - which leads to unfavorable results (see Theorem 5).

Based on the second step of the RHCP (i.e., (10)), the optimum neighbor to visit next is j^* where

$$j^* = \arg \min_{j \in \mathcal{N}_i} J_H(u_j^*, v_j^*). \quad (31)$$

In the case of **RHCP3**, as shown in Fig. 2, above j^* in (31) defines the "Action" that the agent has to take at (current) time t . In other words, the agent a has to leave target i at time t and follow the path $(i, j^*) \in \mathcal{E}$ to visit target j^* .

Remark 5: When constructing the objective function of the **RHCP3**, instead of using the local objective function decomposition given in (18), using a weighted version of it such as

$$\bar{J}_i = \alpha J_i + (1 - \alpha) \sum_{m \in \mathcal{N}_i \setminus \{j\}} J_m, \quad (32)$$

for some fixed $\alpha \in [0, 1]$ is a feasible choice which have been found to be more effective in some numerical examples. An ED-RHC approach where this modified **RHCP3** objective function is used is labeled as ED-RHC $^\alpha$. Also, it should be noted that this modification does not cause any non-trivial changes to the presented theoretical results.

IV. SOLVING THE EVENT-DRIVEN RECEDING HORIZON CONTROL PROBLEM FORM - 2 (**RHCP2**)

As described in Section II, an agent $a \in \mathcal{A}$ residing in target i at some local event time t has to evaluate the **RHCP2** only if the occurred event is: (i) a strictly local $R_i \rightarrow 0^+$ event, or (ii) a neighbor induced event while $R_i(t) = 0$. Therefore, the decision variable u_i of the original RHCP formulation is irrelevant for this case. Hence the **RHCP2** involves only four decision variables: $U_{ij} \triangleq [v_i, u_j, v_j]$ and j (as $u_i^* = 0$ by default in this case). Out of these four, the optimum choice for $v_i = v_i^*$ is taken as the inactive time ahead to be spent at target i .

As shown in Fig. 1 (with $u_i = 0$ and $R_i(t) = 0$), the agent plans to spend an inactive time of v_i on i (starting from the current time t) and then to visit neighbor j to spend an active time of u_j and an inactive time of v_j on j . The variable horizon w in (12) for this case is $w = v_i + \rho_{ij} + u_j + v_j$. Similar to the case with **RHCP3** discussed in the previous section, targets $j \in \mathcal{N}_i$ where $\rho_{ij} > H$ are omitted from evaluating (9) of the **RHCP2** and $\rho_{ij} \leq H$ is assumed.

a) Constraints: Similar to before, u_j and v_j are inter-dependent due to the target j 's uncertainty dynamics (1). Therefore, they follow the physical constraints given in (15). Similarly, target i 's uncertainty dynamics (1) constrain $v_i \geq 0$.

Recall that u_j^B in (15) (i.e., (16)) is the required active time to make $R_j \rightarrow 0$. However, due to the inclusion of v_i , now, u_j^B is dependent on v_i . Therefore, this section uses the notation $u_j^B = u_j^B(v_i)$ where, (using (1), redefining (16))

$$u_j^B(v_i) = \frac{R_j(t + v_i + \rho_{ij})}{B_j - A_j} = \frac{R_j(t) + A_j \rho_{ij}}{B_j - A_j} + \frac{A_j}{B_j - A_j} \cdot v_i. \quad (33)$$

As it will be shown next, the other control limiting parameters (i.e., \bar{v}_i, \bar{u}_j and \bar{v}_j) now become control dependent (i.e., either on v_i, u_j or v_j).

Now, the physical constraints in (15) are developed to incorporate (33) and the horizon constraints (i.e., $w \leq H$) stated above. This defines two classes for feasible $[v_i, u_j, v_j]$ values for the **RHCP2** as follows:

$$\begin{cases} 0 \leq v_i \leq \bar{v}_i(u_j, v_j) \text{ and} \\ \text{Class 1: } 0 \leq u_j \leq \bar{u}_j(v_i) \text{ and } v_j = 0, \text{ or,} \\ \text{Class 2: } u_j = u_j^B(v_i) \text{ and } 0 \leq v_j \leq \bar{v}_j(v_i), \end{cases} \quad (34)$$

where, $u_j^B(v_i)$ is given in (33) and

$$\begin{aligned} \bar{v}_i(u_j, v_j) &= H - (\rho_{ij} + u_j + v_j), \\ \bar{u}_j(v_i) &= \min\{u_j^B(v_i), H - (v_i + \rho_{ij})\}, \\ \bar{v}_j(v_i) &= H - (v_i + \rho_{ij} + u_j^B(v_i)). \end{aligned}$$

Similar to (17), \bar{u}_j and \bar{v}_j respectively represent the limiting values of active and inactive times at j . Along the same lines,

\bar{v}_i is the upper bound to the inactive time at i . However, in contrast to (17), the aforementioned three quantities are control dependent in (34).

Moreover, note that in (34), under Class 1, $\bar{v}_i(u_j, v_j) = \bar{v}_i(u_j, 0)$ and under Class 2, $\bar{v}_i(u_j, v_j) = \bar{v}_i(u_j^B(v_i), v_j)$. Now, any decision $U_{ij} = [v_i, u_j, v_j]$ that follows (34) is feasible for the **RHCP2**, i.e., $U_{ij} \in \mathbb{U}$ in (13).

b) Objective: Following from the generic RHCP objective function definition in (13), the objective function corresponding to the **RHCP2** is taken as $J_H(U_{ij})$ where

$$J_H(U_{ij}) = J_H(X_i(t), [0, U_{ij}]; H) = \frac{1}{w} \bar{J}_i(t, t+w).$$

In order to obtain an expression for J_H , \bar{J}_i in (8) is decomposed as,

$$\bar{J}_i = J_i + J_j + \sum_{m \in \mathcal{N}_i \setminus \{j\}} J_m. \quad (35)$$

Now, each of the above three terms J_i, J_j and J_m should be evaluated for a case where agent a goes from target i to j following the decisions v_i, u_j, v_j during the period $[t, t+w]$. State trajectories for a such situation are shown in Fig. 4. Similar to before, Theorem 1 is utilized for this purpose which gives:

$$\begin{aligned} J_i &= \frac{A_i(\rho_{ij} + u_j + v_j)^2}{2}, \\ J_j &= \frac{(v_i + \rho_{ij})}{2} [2R_j(t) + A_j(v_i + \rho_{ij})] \\ &\quad + \frac{u_j}{2} [2(R_j(t) + A_j(v_i + \rho_{ij})) - (B_j - A_j)u_j], \\ J_m &= \frac{(v_i + \rho_{ij} + u_j + v_j)}{2} [2R_m(t) + A_m(v_i + \rho_{ij} + u_j + v_j)]. \end{aligned}$$

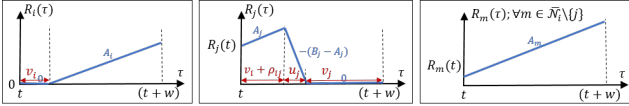


Fig. 4: State trajectories of targets in \mathcal{N}_i during $[t, t+w]$

Now, combining the above three results and substituting it in (35) gives the complete objective function $J_H(U_{ij})$ as

$$J_H(v_i, u_j, v_j) = \frac{[C_1 v_i^2 + C_2 u_j^2 + C_3 v_j^2 + C_4 v_i u_j + C_5 v_i v_j + C_6 u_j v_j + C_7 v_i + C_8 u_j + C_9 v_j + C_{10}]}{v_i + \rho_{ij} + u_j + v_j}, \quad (36)$$

where

$$\begin{aligned} C_1 &= \frac{\bar{A}_i}{2}, \quad C_2 = \frac{\bar{A} - B_j}{2}, \quad C_3 = \frac{\bar{A}_j}{2}, \quad C_4 = \bar{A}_i, \quad C_5 = \bar{A}_{ij}, \\ C_6 &= \bar{A}_j, \quad C_7 = [\bar{R}_i(t) + \bar{A}_i \rho_{ij}], \quad C_8 = [\bar{R}_i(t) + \bar{A}_j \rho_{ij}], \\ C_9 &= [\bar{R}_{ij}(t) + \bar{A}_j \rho_{ij}] \quad \text{and} \quad C_{10} = \frac{\rho_{ij}}{2} [2\bar{R}_i(t) + \bar{A}_j \rho_{ij}]. \end{aligned}$$

The remaining parameters are same as (20). Note that all the coefficients stated above are non-negative except for C_2 , where $C_2 \geq 0 \iff \bar{A} \geq B_j$.

c) Solving the RHCP2 for optimal control (v_i^*, u_j^*, v_j^*) : Based on the first step of the generic RHCP given in (9), the optimal controls for the **RHCP2** are determined by

$$\begin{aligned} (v_i^*, u_j^*, v_j^*) &= \arg \min_{(v_i, u_j, v_j)} J_H(v_i, u_j, v_j) \\ (v_i, u_j, v_j) &\text{ s.t. (34).} \end{aligned} \quad (37)$$

- Class 1: First assume (v_i^*, u_j^*, v_j^*) belongs to the Class 1 defined in (34). Then, $v_j = v_j^* = 0$ and (37) takes the form:

$$\begin{aligned} (v_i^*, u_j^*) &= \arg \min_{(v_i, u_j)} J_H(v_i, u_j, 0) \\ v_i &\geq 0, \\ 0 &\leq u_j \leq u_j^B(v_i), \\ v_i + u_j &\leq H - \rho_{ij}. \end{aligned} \quad (38)$$

The above constraints are a result of the constraints in (34) and the relationships:

$$\begin{aligned} v_i &\leq \bar{v}_i(u_j, 0) \iff v_i \leq H - (\rho_{ij} + u_j), \text{ and,} \\ u_j &\leq \bar{u}_j(v_i) \iff u_j \leq u_j^B(v_i) \ \& \ u_j \leq H - (v_i + \rho_{ij}). \end{aligned}$$

Note that $u_j^B(v_i)$ is linear in v_i (see (33)).

- Class 2: Now, assume (v_i^*, u_j^*, v_j^*) belongs to the Class 2 defined in (34). Then, $u_j = u_j^* = u_j^B(v_i^*)$ and (37) takes the form:

$$\begin{aligned} (v_i^*, v_j^*) &= \arg \min_{(v_i, v_j)} J_H(v_i, u_j^B(v_i), v_j) \\ v_i &\geq 0, \\ v_j &\geq 0, \\ v_i + u_j^B(v_i) + v_j &\leq H - \rho_{ij}. \end{aligned} \quad (39)$$

The last constraint in (39) is a result of (34) and the relationships:

$$\begin{aligned} v_i &\leq \bar{v}_i(u_j^B(v_i), v_j) \iff v_i \leq H - (\rho_{ij} + u_j^B(v_i) + v_j), \text{ and,} \\ v_j &\leq \bar{v}_j(v_i) \iff v_j \leq H - (v_i + \rho_{ij} + u_j^B(v_i)). \end{aligned}$$

- Combined Result: The formulated optimization problems (38) and (39) (even also (21)) directly belongs to the class of *constrained rational function optimization problems* (RFOPs) discussed in Appendix A (see (58)). Specifically, Appendix A presents a computationally cheap theoretical solution developed for such RFOPs.

Upon individually obtaining solutions to (38) and (39), the main optimization problem (37) is solved by just comparing objective function values of individual solutions.

d) Solving for optimal (planned) next destination j^* : The second step of the **RHCP2** (similar to (10)) is to choose the optimum neighbor j according to

$$j^* = \arg \min_{j \in \mathcal{N}_i} J_H(v_i^*, u_j^*, v_j^*). \quad (40)$$

Note that this step requires the cost value of the optimal solution $U_{ij}^{2*} = [v_i^*, u_j^*, v_j^*]$ obtained for each $j \in \mathcal{N}_i$ (in (37)). Now, v_i^* taken from U_{ij}^{2*} defines the “Action” that the agent has to take at current time t . In other words, such v_i^* is the inactive time that the agent should spend on current target i starting from the current time t before leaving.

V. SOLVING THE EVENT-DRIVEN RECEDING HORIZON CONTROL PROBLEM FORM - 1 (**RHCP1**)

An agent $a \in \mathcal{A}$ residing in target i at some local event time t has to evaluate the **RHCP1** only if the occurred event is: (i) the agent a 's own arrival at i , or (ii) a neighbor induced event while $R_i(t) > 0$. Therefore, all the decision variables i.e., $U_{ij} \triangleq [u_i, v_i, u_j, v_j]$ and j of the original RHCP formulation is relevant for this case. Out of these five decisions, the optimum choice for $u_i = u_i^*$ is implemented directly as the active time ahead to be spent at target i - until the next local event occurs.

As shown in Fig. 1, starting from current time t the agent plans to spend active and inactive times first at target i (u_i and v_i respectively) and then at target j (u_j and v_j respectively). The variable horizon w for this case is as (12) where $w = u_i + v_i + \rho_{ij} + u_j + v_j$. Similar to the **RHCP2** and **RHCP3** discussed before, targets $j \in \mathcal{N}_i$ where $\rho_{ij} > H$ are omitted from evaluating (9) of the **RHCP1** and thus $\rho_{ij} \leq H$ is assumed in the following formulation.

a) Constraints: The physical constraints given in (15) are now applied to both targets i and j . In there, u_i^B and u_j^B are respectively used to represent the active time required to make $R_i \rightarrow 0$ and $R_j \rightarrow 0$. While both u_i^B and u_j^B are dependent on the respective initial conditions, target parameters and transit time, u_j^B has an extra dependence on the control decisions u_i and v_i . Hence the notation $u_j^B = u_j^B(u_i, v_i)$ is used in this section. Explicitly, (using (1))

$$\begin{aligned} u_i^B &= \frac{R_i(t)}{B_i - A_i}, \text{ and} \\ u_j^B &= u_j^B(u_i, v_i) = \frac{R_j(t) + A_j \rho_{ij}}{B_j - A_j} + \frac{A_j}{B_j - A_j} \cdot (u_i + v_i). \end{aligned} \quad (41)$$

Now, the physical constraints in (15) are developed to incorporate (41) and the horizon constraints (i.e., $w \leq H$) stated above. This defines four classes named as Class 1A, 1B, 2A and 2B for feasible $[u_i, v_i, u_j, v_j]$ values for the **RHCP1** as follows:

$$\left\{ \begin{array}{l} \text{Class 1: } 0 \leq u_i \leq \bar{u}_i(u_j, v_j) \text{ and } v_i = 0, \text{ or,} \\ \text{Class 2: } u_i = u_i^B \text{ and } 0 \leq v_i \leq \bar{v}_i(u_j, v_j), \end{array} \right\} \times \left\{ \begin{array}{l} \text{Class A: } 0 \leq u_j \leq \bar{u}_j(u_i, v_i) \text{ and } v_j = 0, \text{ or,} \\ \text{Class B: } u_j = u_j^B(u_i, v_i) \text{ and } 0 \leq v_j \leq \bar{v}_j(u_i, v_i), \end{array} \right\} \quad (42)$$

where, u_i^B and $u_j^B(u_i, v_i)$ are given in (41) and

$$\begin{aligned} \bar{u}_i(u_j, v_j) &= \min\{u_i^B, H - (\rho_{ij} + u_j + v_j)\}, \\ \bar{v}_i(u_j, v_j) &= H - (u_i^B + \rho_{ij} + u_j + v_j), \\ \bar{u}_j(u_i, v_i) &= \min\{u_j^B(u_i, v_i), H - (u_i + v_i + \rho_{ij})\}, \\ \bar{v}_j(u_i, v_i) &= H - (u_i + v_i + \rho_{ij} + u_j^B(u_i, v_i)). \end{aligned}$$

Similar to (17) and (34), the notation \bar{u}_j and \bar{v}_j respectively represent the limiting values of active and inactive times feasible at j . And \bar{u}_i and \bar{v}_i represent the same for target i . However, unlike in (17) or (34), each of these four limiting values are now dependent on two control decisions. Now,

any decision $U_{ij} = [u_i, v_i, u_j, v_j]$ that belongs to one of the classes in (42), is feasible for the **RHCP1**, i.e., $U_{ij} \in \mathcal{U}$ in (13).

b) Objective: According to the RHCP objective function given in (13), that of **RHCP1** is taken as $J_H(U_{ij})$ where

$$J_H(U_{ij}) = J_H(X_i(t), U_{ij}; H) = \frac{1}{w} \bar{J}_i(t, t + w).$$

To obtain an expression for $J_H(U_{ij})$, \bar{J}_i (defined in (8)) is decomposed as (35). Next, the three terms J_i , J_j and J_m are evaluated for a case where the agent goes from target i to j following decisions U_{ij} during the period $[t, t + w]$. State trajectories for a such scenario is given in Fig. 5. Theorem 1 is utilized for this purpose to obtain:

$$\begin{aligned} J_i &= \frac{u_i}{2} [2R_i(t) - (B_i - A_i)u_i] + \frac{(\rho_{ij} + u_j + v_j)}{2} \\ &\quad \times [2(R_i(t) - (B_i - A_i)u_i) + A_i(\rho_{ij} + u_j + v_j)], \\ J_j &= \frac{(u_i + v_i + \rho_{ij})}{2} [2R_j(t) + A_j(u_i + v_i + \rho_{ij})] \\ &\quad + \frac{u_j}{2} [2(R_j(t) + A_j(u_i + v_i + \rho_{ij})) - (B_j - A_j)u_j], \\ J_m &= \frac{(u_i + v_i + \rho_{ij} + u_j + v_j)}{2} [2R_m(t) \\ &\quad + A_m(u_i + v_i + \rho_{ij} + u_j + v_j)]. \end{aligned}$$

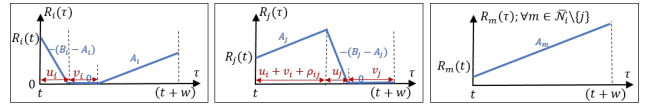


Fig. 5: State trajectories of targets in \mathcal{N}_i during $[t, t + w]$

Now, combining the above three results and substituting it in (35) gives the complete objective function $J_H(U_{ij})$ as

$$\begin{aligned} J_H(u_i, v_i, u_j, v_j) &= \\ &= \frac{C_1 u_i^2 + C_2 v_i^2 + C_3 u_j^2 + C_4 v_j^2 + C_5 u_i v_i}{u_i + v_i + \rho_{ij} + u_j + v_j} \\ &\quad + \frac{C_6 u_i u_j + C_7 u_i v_j + C_8 v_i u_j + C_9 v_i v_j + C_{10} u_i v_j}{u_i + v_i + \rho_{ij} + u_j + v_j} \\ &\quad + \frac{C_{11} u_i + C_{12} v_i + C_{13} u_j + C_{14} v_j + C_{15}}{u_i + v_i + \rho_{ij} + u_j + v_j}, \end{aligned} \quad (43)$$

where

$$\begin{aligned} C_1 &= \frac{\bar{A} - B_i}{2}, \quad C_2 = \frac{\bar{A}_i}{2}, \quad C_3 = \frac{\bar{A} - B_j}{2}, \quad C_4 = \frac{\bar{A}_j}{2}, \\ C_5 &= \bar{A}_i, \quad C_6 = \bar{A} - B_i, \quad C_7 = \bar{A}_j - B_i, \quad C_8 = \bar{A}_i, \\ C_9 &= \bar{A}_{ij}, \quad C_{10} = \bar{A}_j, \quad C_{11} = [\bar{R}(t) + (\bar{A} - B_i)\rho_{ij}], \\ C_{12} &= [\bar{R}_i(t) + \bar{A}_i \rho_{ij}], \quad C_{13} = [\bar{R}(t) + \bar{A} \rho_{ij}], \\ C_{14} &= [\bar{R}_j(t) + \bar{A}_j \rho_{ij}] \text{ and } C_{15} = \frac{\rho_{ij}}{2} [2\bar{R}(t) + \bar{A} \rho_{ij}]. \end{aligned}$$

The remaining parameters are same as (20). Note that all the coefficients stated above are non-negative except for C_1, C_3, C_6, C_7 and C_{11} .

c) **Solving the RHCP1 for optimal control** $(u_i^*, v_i^*, u_j^*, v_j^*)$: The first step of the **RHCP1** can be stated based on (9) and (43) as:

$$(u_i^*, v_i^*, u_j^*, v_j^*) = \underset{(u_i, v_i, u_j, v_j)}{\operatorname{argmin}} J_H(u_i, v_i, u_j, v_j) \quad (44)$$

$$(u_i, v_i, u_j, v_j) \text{ s.t. (42).}$$

- **Class 1A**: First assume $(u_i^*, v_i^*, u_j^*, v_j^*)$ belongs to the Class 1A defined in (42). Then, $v_i = v_i^* = 0$, $v_j = v_j^* = 0$ and (44) takes the form:

$$(u_i^*, u_j^*) = \underset{(u_i, u_j)}{\operatorname{argmin}} J_H(u_i, 0, u_j, 0) \quad (45)$$

$$0 \leq u_i \leq u_i^B,$$

$$0 \leq u_j \leq u_j^B(u_i, 0),$$

$$u_i + u_j \leq H - \rho_{ij}.$$

To write the constraints in (45), (42) and the relationships:

$$u_i \leq \bar{u}_i(u_j, 0) \iff u_i \leq u_i^B \text{ \& } u_i \leq H - (\rho_{ij} + u_j), \text{ and,}$$

$$u_j \leq \bar{u}_j(u_i, 0) \iff u_j \leq u_j^B(u_i, 0) \text{ \& } u_j \leq H - (u_i + \rho_{ij}),$$

have been used. Note that $u_j^B(u_i, 0)$ is linear and increasing with u_i (see (41)).

- **Class 1B**: Now assume $(u_i^*, v_i^*, u_j^*, v_j^*)$ belongs to the Class 1B defined in (42). Then, $v_i = v_i^* = 0$, $u_j = u_j^* = u_j^B(u_i^*, 0)$ and (44) takes the form:

$$(u_i^*, v_j^*) = \underset{(u_i, v_j)}{\operatorname{argmin}} J_H(u_i, 0, u_j^B(u_i, 0), v_j) \quad (46)$$

$$0 \leq u_i \leq u_i^B,$$

$$v_j \geq 0,$$

$$u_i + u_j^B(u_i, 0) + v_j \leq H - \rho_{ij}.$$

The constraints in (46) are from (42) and the relationships:

$$u_i \leq \bar{u}_i(u_j^B(u_i, 0), v_j) \iff$$

$$u_i \leq u_i^B \text{ \& } u_i \leq H - (\rho_{ij} + u_j^B(u_i, 0) + v_j), \text{ and,}$$

$$v_j \leq \bar{v}_j(u_i, 0) \iff v_j \leq H - (u_i + \rho_{ij} + u_j^B(u_i, 0)).$$

- **Class 2A**: Now assume $(u_i^*, v_i^*, u_j^*, v_j^*)$ belongs to the Class 2A defined in (42). Then, $u_i = u_i^* = u_i^B$, $v_j = v_j^* = 0$ and (44) takes the form:

$$(v_i^*, u_j^*) = \underset{(v_i, u_j)}{\operatorname{argmin}} J_H(u_i^B, v_i, u_j, 0) \quad (47)$$

$$v_i \geq 0,$$

$$0 \leq u_j \leq u_j^B(u_i^B, v_i),$$

$$v_i + u_j \leq H - (u_i^B + \rho_{ij}).$$

The constraints in (47), are from (42) and the relationships:

$$v_i \leq \bar{v}_i(u_j, 0) \iff v_i \leq H - (u_i^B + \rho_{ij} + u_j), \text{ and,}$$

$$u_j \leq \bar{u}_j(u_i^B, v_i) \iff$$

$$u_j \leq u_j^B(u_i^B, v_i) \text{ \& } u_j \leq H - (u_i^B + v_i + \rho_{ij}).$$

Note that $u_j^B(u_i^B, v_i)$ is linear and increasing with v_i (41).

- **Class 2B**: Now, assume $(u_i^*, v_i^*, u_j^*, v_j^*)$ belongs to the Class 2B defined in (42). Then, $u_i = u_i^* = u_i^B$, $u_j = u_j^* = u_j^B(u_i^B, v_i^*)$, and (37) takes the form:

$$(v_i^*, v_j^*) = \underset{(v_i, v_j)}{\operatorname{argmin}} J_H(u_i^B, v_i, u_j^B(u_i^B, v_i), v_j) \quad (48)$$

$$v_i \geq 0,$$

$$v_j \geq 0,$$

$$v_i + v_j + u_j^B(u_i^B, v_i) \leq H - (u_i^B + \rho_{ij}).$$

To write the last constraint in (48), (42) and the relationships:

$$v_i \leq \bar{v}_i(u_j^B(u_i^B, v_i), v_j) \iff$$

$$v_i \leq H - (u_i^B + \rho_{ij} + u_j^B(u_i^B, v_i) + v_j), \text{ and,}$$

$$v_j \leq \bar{v}_j(u_i^B, v_i) \iff v_j \leq H - (u_i^B + v_i + \rho_{ij} + u_j^B(u_i^B, v_i)),$$

have been used.

- **Combined Result**: The optimization problems (45), (46), (47) and (48) formulated above belong to the class of constrained rational function optimization problems (58) discussed in Appendix A (similar to (38), (39) and (21)). Therefore, each of these four problems are solved exploiting the computationally cheap theoretical solution presented in Appendix B.

Upon obtaining solutions to (45)-(48), the main optimization problem (44) is solved by just comparing objective function values of the obtained individual solutions.

d) **Solving for optimal (planned) next destination j^*** : The second step of the **RHCP1** (same as (10)) is to choose the optimum neighbor j according to

$$j^* = \underset{j \in \mathcal{N}_i}{\operatorname{argmin}} J_H(u_i^*, v_i^*, u_j^*, v_j^*). \quad (49)$$

Note that this step requires the cost value of the optimal solution $U_{ij}^* = [u_i^*, v_i^*, u_j^*, v_j^*]$ obtained for each $j \in \mathcal{N}_i$ (in (44)). As shown in Fig. 2, u_i^* chosen from U_{ij}^* defines the "Action" that the agent has to take at $t = t$. In other words, such u_i^* (depends on j^*) is the active time that the agent should spend on current target i - until the next local event occurs.

VI. SIMULATION RESULTS

This section compares the performance (i.e., J_T in (2)) obtained for several different persistent monitoring problem configurations using: (i) the proposed event-driven receding horizon control (ED-RHC) method, (ii) the RD-RHC $^\alpha$ method suggested in Remark 5, and (iii) the infinitesimal perturbation analysis based threshold control policy (IPA-TCP) method proposed in [5]. Note that all three methods: ED-RHC, ED-RHC $^\alpha$ and IPA-TCP solutions are on-line and distributed (in contrast to the off-line and centralized solution proposed in [6]). All three of these solutions have been implemented in a JavaScript based simulator, which is made available at <http://www.bu.edu/codes/simulations/shiran27/PersistentMonitoring/>. Readers are invited to reproduce the reported results and also to try new problem configurations using the developed interactive simulator.

Specifically, this section considers the four single-agent problem configurations shown in Figs. 7-10 and the four multi-agent problem configurations shown in Fig. 11-14. In each problem configuration diagram, blue circles represent the targets, while black lines represent available path segments that agents can take to travel between targets. Red triangles and the yellow vertical bars indicate the agent locations and the target uncertainty levels, respectively. Moreover, since both of those quantities are time-varying (i.e., $s_a(t)$ and $R_i(t)$), in figures, their state at the terminal time $t = T$ is shown (upon using either ED-RHC or IPA-TCP solution in the simulation).

In each problem configuration, the used problem parameters are as follows. The target parameters were chosen as $A_i = 1$, $B_i = 10$ and $R_i(0) = 0.5$, $\forall i \in \mathcal{T}$. Also, the used target location co-ordinates (i.e., Y_i) are specified in each problem configuration figure. Note that in all the examples, all the targets have been placed inside a 600×600 mission space. The interested time period was taken as $T = 500$. Each agent's maximum speed was taken as 50 units per second. The initial locations of the agents were chosen such that they are uniformly distributed among the targets at $t = 0$ (i.e., $s_a(0) = Y_i$ with $i = 1 + (a - 1) * \text{round}(M/N)$). The fixed planning horizon H was chosen as $H = 250$ for the two ED-RHC approaches and $\alpha = 0.05$ was used for the ED-RHC $^\alpha$.

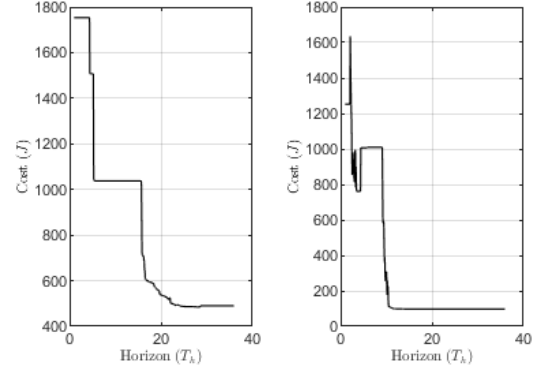
Each sub-figure caption (in Figs. 7-14) provides the cost value (i.e., J_T in (2)) observed under the used controller (i.e., either ED-RHC, ED-RHC $^\alpha$ or IPA-TCP). These cost values are summarized in Tab. I. For the problem configurations shown in Fig. 10 and 14, the respective sub-figures in Fig. 6 shows the performance of the ED-RHC solution (i.e., J_T) under different fixed planning horizon values (i.e., H). In each case, the optimum time horizon value and its corresponding (minimum) cost value are indicated in the respective sub-figure caption.

From Tab. I, note that the proposed ED-RHC method has performed considerably better (on average 50.4% better) than the IPA-TCP method for multi-agent problem configurations. Also, for single-agent problem configurations, both methods have performed equally. The proposed ED-RHC $^\alpha$ approach (in Remark 5) further improves these performances compared to the IPA-TCP method: on average by 67.2% for multi-agent situations and by 2.76% for single agent situations.

Cost J_T vs. fixed planning horizon H plots shown in 6 implies that having a large enough time horizon can directly give a performance level that is very closer to the optimum (within 1.1%). Hence, there is no evident importance of attempting to fine-tune the H value. Moreover, note that the complexity of the ED-RHC solution is invariant to the H value. This highlights the impact of our main contribution of introducing a variable horizon so as to determine the optimal horizon at each instance where the RHCP is solved.

TABLE I: Summary of obtained results across all the simulation examples.

J_T in (2)	Single Agent Simulation Examples				Multi-Agent Simulation Examples			
	1	2	3	4	1	2	3	4
IPA-TCP	22.9	47.1	129.2	497.9	270.2	91.7	274.0	201.3
ED-RHC	22.4	47.1	141.4	490.4	105.5	63.7	114.1	97.2
ED-RHC $^\alpha$	22.9	47.1	121.4	473.2	95.4	39.0	64.8	61.0



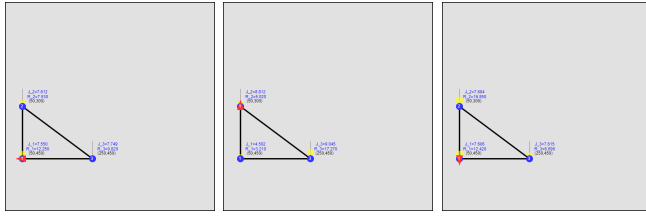
(a) SASE 4
Min Cost: $J_T = 484.1$ at
Horizon: $H = 12.27$.

(b) MASE 4
Min Cost: $J_T = 96.1$ at
Horizon: $H = 12.27$.

Fig. 6: Cost J_T vs horizon H plot for SASE4 and MASE4.

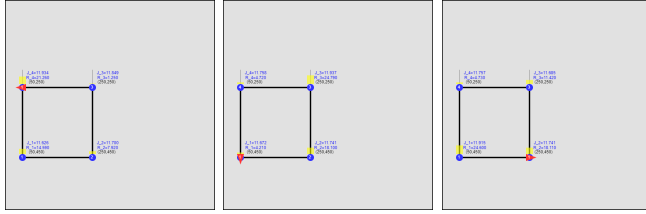
VII. CONCLUSION

This paper considers the optimal multi-agent persistent monitoring problem defined on a set of targets interconnected according to a fixed graph topology. Departing from existing computationally expensive and slow threshold-based parametric control solutions, a novel computationally efficient and robust event-driven receding horizon control solution is proposed. Specifically, we simultaneously determine both a locally optimal trajectory and optimal planning horizon for each agent at different discrete event times on its trajectory. Numerical results show significant improvements compared to the existing parametric control solutions. Ongoing work is aimed to combine time-driven features of parametric control strategies with the proposed ED-RHC approach to construct a hybrid optimal control solution to the PMG problem.



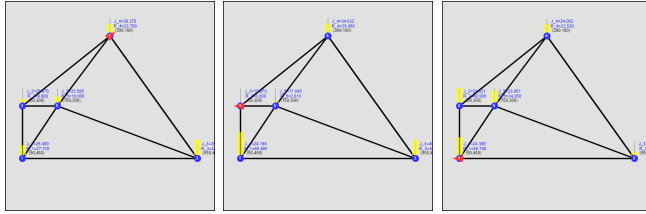
(a) IPA-TCP: $J_T = 22.9$.
(b) ED-RHC: $J_T = 22.4$.
(c) ED-RHC $^\alpha$: $J_T = 22.9$.

Fig. 7: Single-agent simulation example 1 (SASE1) with 3 targets (state shown at terminal time $t = T$).



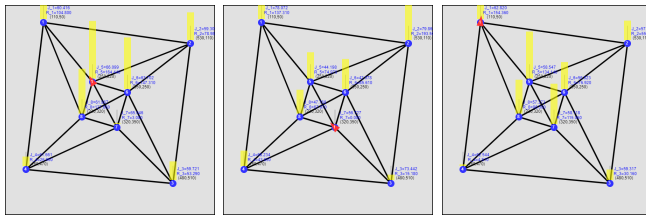
(a) IPA-TCP: $J_T = 47.1$.
(b) ED-RHC: $J_T = 47.1$.
(c) ED-RHC $^\alpha$: $J_T = 47.1$.

Fig. 8: Single-agent simulation example 2 (SASE2) with 4 targets (state shown at terminal time $t = T$).



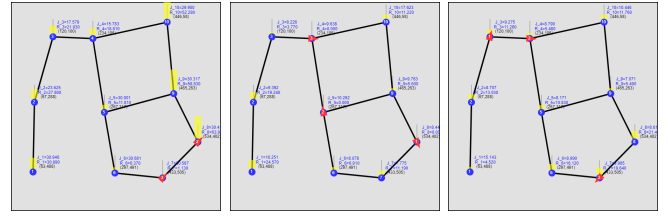
(a) IPA-TCP: $J_T = 129.2$.
(b) ED-RHC: $J_T = 141.4$.
(c) ED-RHC $^\alpha$: $J_T = 121.4$.

Fig. 9: Single-agent simulation example 3 (SASE3) with 5 targets (state shown at terminal time $t = T$).



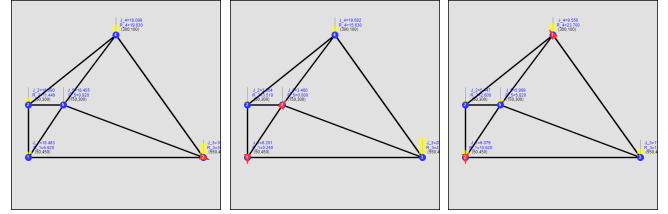
(a) IPA-TCP: $J_T = 497.9$.
(b) ED-RHC: $J_T = 490.4$.
(c) ED-RHC $^\alpha$: $J_T = 473.2$.

Fig. 10: Single-agent simulation example 4 (SASE4) with 8 targets (state shown at terminal time $t = T$).



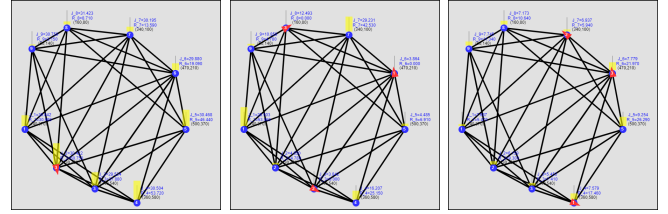
(a) IPA-TCP: $J_T = 270.2$.
(b) ED-RHC: $J_T = 105.5$.
(c) ED-RHC $^\alpha$: $J_T = 95.4$.

Fig. 11: Multi-agent simulation example 1 (MASE1) with 3 agents and 9 targets (state shown at terminal time $t = T$).



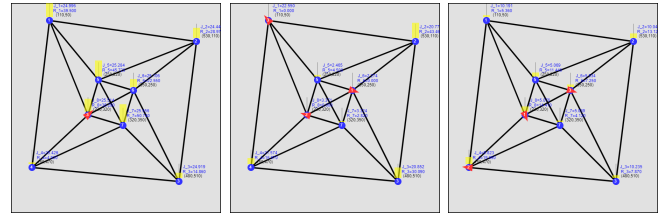
(a) IPA-TCP: $J_T = 91.7$.
(b) ED-RHC: $J_T = 63.7$.
(c) ED-RHC $^\alpha$: $J_T = 39.0$.

Fig. 12: Multi-agent simulation example 2 (MASE2) with 2 agents and 5 targets (state shown at terminal time $t = T$).



(a) IPA-TCP: $J_T = 274.0$.
(b) ED-RHC: $J_T = 114.1$.
(c) ED-RHC $^\alpha$: $J_T = 64.8$.

Fig. 13: Multi-agent simulation example 3 (MASE3) with 3 agents and 9 targets (state shown at terminal time $t = T$).



(a) IPA-TCP: $J_T = 201.3$.
(b) ED-RHC: $J_T = 97.2$.
(c) ED-RHC $^\alpha$: $J_T = 61.0$.

Fig. 14: Multi-agent simulation example 4 (MASE4) with 3 agents and 8 targets (state shown at terminal time $t = T$).

APPENDIX

A. Constrained optimization of bivariate rational functions

a) **Convexity of rational functions:** Consider a rational function $h: \mathbb{R} \rightarrow \mathbb{R}$ of the form $h(r) = \frac{f(r)}{g(r)}$ and assume $g(r) > 0$, $\forall r \in \mathcal{U} \subseteq \mathbb{R}$ where \mathcal{U} is a closed interval. In the following discussion, when writing $f(r)$, $g(r)$ or $h(r)$, their argument

is omitted for notational convenience. Also, the notation “ $'$ ” is used to denote the derivative of a function with respect to r .

Lemma 3: Whenever $g(r)$ and $f(r)$ polynomials satisfy

$$g[gf''' - fg'''] - 3g''[gf' - fg'] = 0, \quad \forall r \in \mathcal{U}, \quad (50)$$

$h(r)$ is convex (or concave) on \mathcal{U} if $\Delta_h(r_0) > 0$ (or $\Delta_h(r_0) < 0$) where $r_0 \in \mathcal{U}$ and

$$\Delta_h(r) \triangleq g[gf'' - fg''] - 2g'[gf' - fg']. \quad (51)$$

Proof: The first and second order derivatives of $h(r)$ can be written respectively as as

$$h' = \frac{gf' - fg'}{g^2} \text{ and } h'' = \frac{g[gf'' - fg''] - 2g'[gf' - fg']}{g^3}.$$

Note that $h''(r) = \frac{\Delta_h(r)}{g^3(r)}$ and $g^3(r) > 0, \forall r \in \mathcal{U}$. Therefore, convexity of $h(r)$ will only depend on the condition:

$$h''(r) > 0, \forall r \in \mathcal{U} \iff \Delta_h(r) > 0, \forall r \in \mathcal{U}.$$

This condition is easily satisfied whenever

$$\Delta_h(r_0) > 0 \text{ for some } r_0 \in \mathcal{U} \text{ and } \Delta_h'(r) = 0 \text{ for all } r \in \mathcal{U}.$$

Finally, deriving $\Delta_h'(r)$ which yields the expression in (50)

$$\Delta_h'(r) = g[gf''' - fg'''] - 3g''[gf' - fg'],$$

completes the proof. \blacksquare

Remark 6: The condition given in (50) (in Lemma 3) is a sufficient condition for the convexity (or concavity) of $h(r)$ on \mathcal{U} . As an example, it is satisfied whenever the denominator polynomial $g(r)$ is of first degree and the numerator polynomial $f(r)$ is of second degree.

b) Constrained minimization of $h(r)$: Assume $h(r)$ to be a rational function which satisfies the conditions discussed above: $g(r) > 0, \Delta_h'(r) = 0, \forall r \in \mathcal{U} \subseteq \mathbb{R}$. Further, assume the signs of $\Delta_h(r_0)$ and $h'(r_0)$ are known at some point of interest $r = r_0 \in \mathcal{U}$ (recall that the sign of $\Delta_h(r_0)$ mimics the sign of $h''(r), r \in \mathcal{U}$). According to Lemma 3, the latter assumption fully determines the convexity (or concavity) of $h(r)$ on \mathcal{U} and its gradient direction at $r = r_0$, respectively. Now, consider the following optimization problem:

$$\begin{aligned} r^* &= \underset{r}{\operatorname{argmin}} h(r) \\ r_0 &\leq r \leq r_1, \end{aligned} \quad (52)$$

where the constrained interval: $[r_0, r_1] \subseteq \mathcal{U}$. A critical r value $r = r^\#$ (which is important to the analysis) is defined as

$$r^\# \triangleq \begin{cases} \{r : h'(r) = 0, r > r_0\} & \text{if } \Delta_h(r_0) > 0 \text{ \& } h'(r_0) < 0, \\ \{r : h(r) = h(r_0), r > r_0\} & \text{if } \Delta_h(r_0) < 0 \text{ \& } h'(r_0) > 0. \end{cases} \quad (53)$$

Note that the the two cases considered above are the only cases where a stationary point of $h(r)$ could occurs for some $r > r_0, r \in \mathcal{U}$ (see also Fig. 15).

Lemma 4: The optimal solution to (52) is as follows:

If $\Delta_h(r_0) < 0$ & $h'(r_0) > 0$

$$r^* = \begin{cases} r_1 & \text{if } r_1 > r^\# \\ r_0 & \text{otherwise,} \end{cases}$$

else if $\Delta_h(r_0) > 0$ & $h'(r_0) < 0$

$$r^* = \begin{cases} r^\# & \text{if } r_1 > r^\# \\ r_1 & \text{otherwise,} \end{cases}$$

otherwise,

$$r^* = \begin{cases} r_0 & \text{if } \Delta_h(r_0) \geq 0 \text{ \& } h'(r_0) \geq 0 \\ r_1 & \text{otherwise.} \end{cases}$$

Proof: The proof is supported by the Fig. 15. \blacksquare

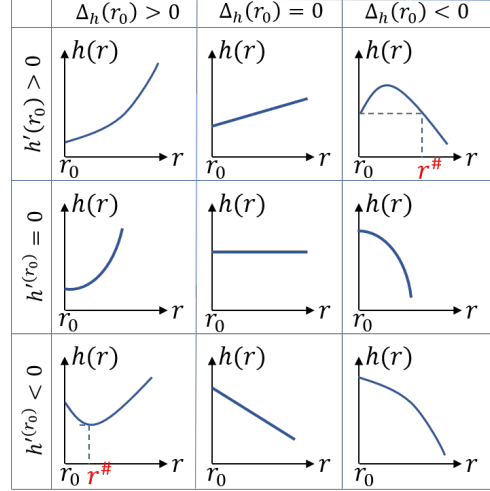


Fig. 15: Graphs of possible $\{h(r) : r \geq r_0, r \in \mathcal{U}\}$ profiles for different cases of $h'(r_0)$ and $\Delta_h(r_0)$ (recall $\operatorname{sgn}(\Delta_h(r_0)) = \operatorname{sgn}(h''(r))$ determines the convexity or concavity).

In essence, an optimization problem of the form (52) can be solved purely based on the numerical values: $h'(r_0)$, $\Delta_h(r_0)$ and $r^\#$. Note that $r^\#$ is only required in two special cases and for the application example mentioned in Remark 6, it can be obtained simply by solving for the roots of a quadratic expression (single variable).

c) Bivariate rational functions: Next, consider the class of *bivariate rational functions* that can be represented by a function $H : \mathbb{R}_+^2 \rightarrow \mathbb{R}$ of the form

$$H(x, y) = \frac{F(x, y)}{G(x, y)} = \frac{C_1x^2 + C_2y^2 + C_3xy + C_4x + C_5y + C_6}{C_7x + C_8y + C_9}, \quad (54)$$

where the coefficients (i.e., $C_1, C_2, C_3, C_4, C_5, C_6, C_7, C_8, C_9$) are known scalar constants with $C_7 \geq 0, C_8 \geq 0$ and $C_9 > 0$. Note that the range space of $H(x, y)$ is limited to the non-negative orthant of \mathbb{R}^2 (denoted by \mathbb{R}_+^2).

Developing conditions for the convexity of $H(x, y)$ is complex. Even if such conditions were derived, interpreting them and exploiting them to solve a two dimensional constrained optimization problem that involves minimizing $H(x, y)$ (analogous to (52)) is doubtful. To address this, the behavior of $H(x, y)$ is proposed to be studied along generic line segments.

Consider a line segment of the form $y = mx + b$ starting at some point $(x_0, y_0) \in \mathbb{R}_+^2$ as shown in Fig. 16. A parameter r is used to represent a generic location (x_r, y_r) on this line

as $(x_r, y_r) = (x_0 + r, y_0 + mr)$ where r have been introduced exploiting the gradient m of the line segment:

$$\frac{y_r - y_0}{x_r - x_0} = m \implies \frac{y_r - y_0}{m} = \frac{x_r - x_0}{1} = r. \quad (55)$$

A rational function $h(r)$ can now be defined as

$$h(r) \triangleq H(x_0 + r, y_0 + mr) = \frac{F(x_0 + r, y_0 + mr)}{G(x_0 + r, y_0 + mr)} = \frac{f(r)}{g(r)}, \quad (56)$$

to represent the $H(x, y)$ along the interested line segment.

The parameter r is constrained such that $r \in \mathcal{U} \triangleq [-x_0, \frac{-y_0}{m}]$ to limit the line segment to \mathbb{R}_+^2 . This allows $h(r)$ to fall directly into the category of rational functions discussed before (i.e., in Lemma 3 and in Remark 6).

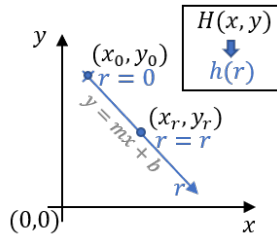


Fig. 16: $H(x, y)$ along the line $y = mx + b$

Theorem 3: The rational function $h(r)$, $r \in \mathcal{U}$ defined in (56) is convex (or concave) if $\Delta_h(r_0) > 0$ (or $\Delta_h(r_0) < 0$), where $r_0 \in \mathcal{U}$ and $\Delta_h(r)$ is defined in (51).

Proof: According to (56) and \mathcal{U} defined above, the denominator polynomial $g(r) = G(x_0 + r, y_0 + mr) > 0$ for all $r \in \mathcal{U}$ as $C_7 \geq 0, C_8 \geq 0$ and $C_9 > 0$ in (54).

Since $g(r)$ and $f(r)$ are polynomials of degree 1 and 2 respectively, they satisfy the condition (50). Thus, Lemma 3 is applicable for $h(r)$ (defined in (56)). Hence, its convexity will depend on the condition $\Delta_h(r_0) > 0$. ■

It is worth pointing out that $\Delta_h(r)$ is in fact independent of r as $\Delta'_h(r) = 0, \forall r \in \mathcal{U}$ (see the last step of the proof of Lemma 3 and (50)). However, it will depend on other parameters (found in (54)) including x_0, y_0 and m . For example, when the line segment defined by $x_0 = 0, y_0 = 0, m = 0$ (i.e., the x -axis) is used, $\Delta_h(r) = 2FG^2 - 2DGK + 2AK^2, \forall r \in \mathbb{R}_+$.

In the introduced parametrization scheme above, the parameter r represents the distance along the x axis from x_0 (projected from the line segment $y = mx + b$). However, if $H(x, y)$ needs to be studied along the y axis (from y_0 projected from a line segment $x = ny + c$), using

$$\frac{y_r - y_0}{x_r - x_0} = \frac{1}{n} \implies \frac{y_r - y_0}{1} = \frac{x_r - x_0}{n} = r, \quad (57)$$

is more appropriate as it gives $(x_r, y_r) = (x_0 + nr, y_0 + r)$.

Above Theorem 3 enables determining the optimum $H(x, y)$ value along a known line segment (on \mathbb{R}_+^2) - using the established Lemma 4 for a problem of the form (52). This capability is exploited next.

d) Constrained minimization of $H(x, y)$: The main objective of this discussion is to obtain a closed form solution to a constrained optimization problem of the form

$$\begin{aligned} (x^*, y^*) &= \underset{(x, y)}{\operatorname{argmin}} H(x, y) \\ x &\geq 0, \\ y &\geq 0, \\ y - \mathbf{P}x &\leq \mathbf{L}, \\ y + \mathbf{Q}x &\leq \mathbf{M}, \\ x &\leq \mathbf{N}, \end{aligned} \quad (58)$$

where $H(x, y)$ is a known bivariate rational function of the form (54) and $\mathbf{P}, \mathbf{Q}, \mathbf{L}, \mathbf{M}$ are known positive constants. These constraints define a convex 2-Polytope as shown in Fig. 17. The steps followed to solve the above problem are discussed next.

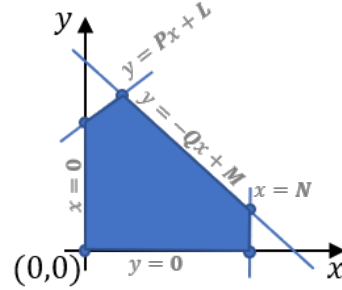


Fig. 17: Feasible space for $H(x, y)$ in (58)

- Step 1: The unconstrained version of (58) is considered first. This is solved using the KKT necessary conditions [15] which reveals two equations of generic conics [16]. Therefore, the stationary points of $H(x, y)$ lies at the (four) intersection points of those two conics. The problem of determining the intersection of two conics boils down to solving a quartic equation which has a well known closed form solution [17]. These (four) solutions are computed and stored in a *solution pool* if they satisfy the constraints.

- Step 2: Next, the constrained version of (58) is considered. In such a case, it is possible for (x^*, y^*) to lie on a constraint. To capture such situations, $H(x, y)$ is optimized along each of the boundary line segments of the feasible space (there are five of them as shown in Fig. 17).

On a selected boundary line segment, the first step is to parametrize $H(x, y)$ to obtain a single variable rational function $h(r)$ (following either (55) or (57)). Then, the next step is to solve the arising convex (or concave) optimization problem (of the form (52)) using Lemma 4. Note that this is enabled by Theorem 3. Finally, the obtained optimum solution is added to the solution pool.

- Step 3: The final step is to pick the best solution out of the solution pool (which only contains at most nine candidates solutions). Therefore, this is achieved by directly evaluating $H(x, y)$ and comparing them for each candidate solution.

This approach is computationally cheap and accurate compared to gradient based methods (which are susceptible to local optima). This concludes the discussion on how to solve a generic problem of the form (58).

B. Omitting the denominator of the RHCP objective function

In this section, the case where the RHCP objective function J_H takes the form

$$J_H(X_i(t), U_{ij}; H) = \bar{J}_i(t, t+w),$$

is investigated where the denominator term w found in the original definition of J_H in (13) is omitted. The main focus here is given to the **RHCP3** where now the objective function $J_H(u_j, v_j)$ takes the form

$$J_H(u_j, v_j) = C_1 u_j^2 + C_2 v_j^2 + C_3 u_j v_j + C_4 u_j + C_5 v_j + C_6.$$

Each coefficient above is same as in (19). In this appendix, it is shown that the above objective function leads to a spurious policy (for j^*).

The first step of **RHCP3** (i.e., (9)) can be stated as:

$$\begin{aligned} (u_j^*, v_j^*) &= \arg \min_{(u_j, v_j)} J_H(u_j, v_j) \\ (u_j, v_j) &\text{ s.t. (17).} \end{aligned} \quad (59)$$

a) **Solving (59) for optimal control** (u_j^*, v_j^*) :

- **Class 1:** First assume (u_j^*, v_j^*) belongs to the Class 1 defined in (17). Then, $v_j^* = 0$ and (59) takes the form: (which also determines u_j^*)

$$\begin{aligned} u_j^* &= \arg \min_{u_j} J_H(u_j, 0) \\ 0 &\leq u_j \leq \bar{u}_j. \end{aligned} \quad (60)$$

Lemma 5: The optimal solution for (60) is

$$u_j^* = 0. \quad (61)$$

Proof: Substituting $v_j = 0$ in (19) gives $J_H(u_j, 0)$ as

$$J_H(u_j, 0) = C_1 u_j^2 + C_4 u_j + C_6. \quad (62)$$

Recall $C_4 \geq 0$, $C_6 \geq 0$ and $C_1 = \frac{1}{2}(\bar{A} - B_j)$.

First, consider the case where $C_1 = 0$. Then, $J_H(u_j, 0)$ is linear in u_j . Also it will have a non-negative gradient as $C_4 \geq 0$. Therefore, when $C_1 = 0$, clearly the constrained optimum is at $u_j^* = 0$.

Note that when $C_1 \neq 0$, the unconstrained optimum of $J_H(u_j, 0)$ is at $u_j = u_j^\# = \frac{-C_4}{2C_1}$ (using calculus). Also note that due to the quadratic nature of $J_H(u_j, 0)$, it should be symmetric around $u_j = u_j^\#$.

As the second case, consider $C_1 > 0$. Then, $J_H(u_j, 0)$ is convex and $u_j^\# \leq 0$. Therefore, when $C_1 > 0$, $u_j^* = 0$.

Finally, consider the case where $C_1 < 0$. Then, $J_H(u_j, 0)$ is concave and $u_j^\# \geq 0$. In this case, using the aforementioned symmetry, the constrained optimum u_j^* can be written as

$$u_j^* = \begin{cases} \bar{u}_j & \text{if } 2u_j^\# < \bar{u}_j \\ 0 & \text{otherwise,} \end{cases} \quad (63)$$

Now, it is required to prove that the condition $2u_j^\# < \bar{u}_j$ never occurs (whenever $C_1 < 0$). Using (19), $u_j^\#$ can be written as,

$$u_j^\# = \frac{-C_4}{2C_1} = \frac{\bar{R}(t) + \bar{A}\rho_{ij}}{B_j - \bar{A}}. \quad (64)$$

Note that $C_1 < 0 \iff B_j \geq \bar{A}$. Also from (19), $R_i(t) \leq \bar{R}(t)$ and $A_i \leq \bar{A}$. Therefore, the denominator and the numerator of $u_j^\#$ above can be bounded as

$$[\bar{R}(t) + \bar{A}\rho_{ij}] \geq [R_j(t) + A_j\rho_{ij}] \text{ and } (B_j - \bar{A}) \leq (B_j - A_j).$$

The above result gives (also using \bar{u}_j, u_j^B definitions in (17)),

$$u_j^\# = \frac{\bar{R}(t) + \bar{A}\rho_{ij}}{B_j - \bar{A}} \geq \frac{R_j(t) + A_j\rho_{ij}}{B_j - A_j} = u_j^B \geq \bar{u}_j. \quad (65)$$

Therefore, $u_j^\# \geq \bar{u}_j$ and hence the condition $2u_j^\# < \bar{u}_j$ in (68) does not hold. Thus, even when $C_1 < 0$, $u_j^* = 0$. This completes the proof. ■

- **Class 2:** Now, assume (u_j^*, v_j^*) belongs to the Class 2 defined in (17). Then, $u_j = u_j^* = u_j^B$ and $0 \leq v_j \leq \bar{v}_j$. Therefore, (59) takes the form: (which also determines v_j^*)

$$\begin{aligned} v_j^* &= \arg \min_{v_j} J_H(u_j^B, v_j) \\ 0 &\leq v_j \leq \bar{v}_j. \end{aligned} \quad (66)$$

Lemma 6: The optimal solution for (66) is

$$v_j^* = 0. \quad (67)$$

Proof: Substituting $u_j = u_j^B$ in (19) gives $J_H(u_j^B, v_j)$ as

$$J_H(u_j^B, v_j) = C_2 v_j^2 + [C_3 u_j^B + C_5] v_j + [C_1 (u_j^B)^2 + C_4 u_j^B + C_6]. \quad (68)$$

Recall $C_2, C_3, C_5, u_j^B \geq 0$ and $C_2 = \frac{\bar{A}_j}{2} = \frac{1}{2} \sum_{m \in \mathcal{N}_i \setminus \{j\}} A_m$.

If $C_2 = 0$, the objective $J_H(u_j^B, v_j)$ is linear in v_j . Also its gradient is non-negative. Therefore, when $C_2 = 0$, clearly the constrained optimum is at $v_j^* = 0$.

Now, consider the case where $C_2 > 0$. Then $J_H(u_j^B, v_j)$ has its unconstrained optimum is at $v_j = v_j^\#$ where

$$v_j^\# = \frac{-[C_3 u_j^B + C_5]}{2C_2},$$

(using calculus). Also note that due to the quadratic nature of $J_H(u_j^B, v_j)$, it should also be symmetric around $v_j = v_j^\#$.

Since $C_2 > 0$, $J_H(u_j^B, v_j)$ is convex. Also, $v_j^\# \leq 0$ as $C_3, C_5, u_j^B \geq 0$. This implies that the constrained optimum is at $v_j^* = 0$ even when $C_2 > 0$. This completes the proof. ■

- **Combined Result:**

Theorem 4: The optimal solution of (59) is $u_j^* = 0$, $v_j^* = 0$, and the optimal cost is $J_H(u_j^*, v_j^*) = C_6$.

Proof: Assume the optimal solution of (59) (u_j^*, v_j^*) belongs to Class 1 of (17). Then, Lemma 5 gives that $u_j^* = 0$, $v_j^* = 0$. The corresponding objective function value (using (62)) is

$$[J_H(u_j^*, v_j^*)]_{\text{Class1}} = C_6.$$

However, if the the optimal solution of (59) is assumed to be in Class 2 of (17), Lemma 6 gives that $u_j^* = u_j^B$, $v_j^* = 0$. The corresponding objective function value (using (68)) is

$$[J_H(u_j^*, v_j^*)]_{Class2} = [C_1(u_j^B)^2 + C_4u_j^B + C_6].$$

If Class 2 to is better performing compared to Class 1,

$$C_1(u_j^B)^2 + C_4u_j^B + C_6 \leq C_6.$$

Using $u_j^B \geq 0$, above condition can be simplified into: $C_1u_j^B + C_4 \leq 0$, which is only possible when $C_1 < 0$ as $C_4 \geq 0$. Therefore, this condition can be simplified as: $C_1 < 0$ and,

$$\frac{-C_4}{C_1} \leq u_j^B.$$

Using (64), the above condition can be written as $2u_j^\# \leq \bar{u}_j$. however, (65) shows that whenever $C_1 \leq 0$, $u_j^\# \geq \bar{u}_j$. Thus, clearly the condition $2u_j^\# \leq \bar{u}_j$ does not hold (A contradiction).

Therefore, the optimal solution of (59) belongs to Class 1 and hence $u_j^* = 0$, $v_j^* = 0$ and $J_H(u_j^*, v_j^*) = C_6$. ■

As a result of the above theorem, when the agent a is ready to leave target i at $t = t$, it can compute the optimal trajectory costs $J_H(u_j^*, v_j^*)$ for all $j \in \mathcal{N}_i$ by simply using the expression for C_6 where

$$J_H(u_j^*, v_j^*) = C_6 = \frac{\rho_{ij}}{2} [2\bar{R}(t) + \bar{A}\rho_{ij}]. \quad (69)$$

b) Solving for optimal next destination j^* : The second step of the **RHCP3** (i.e., (10)) is to choose the optimum neighbor j according to

$$j^* = \arg \min_{j \in \mathcal{N}_i} J_H(u_j^*, v_j^*). \quad (70)$$

As shown in (1), above j^* defines the “Action” that the agent has to take at $t = t$.

Theorem 5: The optimal solution to (70) is the neighbor $j = j^* \in \mathcal{N}_i$ whom can be reached in a shortest time, i.e.,

$$j^* = \arg \min_{j \in \mathcal{N}_i} \rho_{ij}.$$

Proof: The objective function of the discrete optimization problem (70) is (69). Therefore,

$$j^* = \arg \min_{j \in \mathcal{N}_i} \frac{\rho_{ij}}{2} [2\bar{R}(t) + \bar{A}\rho_{ij}].$$

Note that $\bar{R}(t)$ and \bar{A} terms are independent of j (see (19)). Therefore, the above objective function (i.e., C_6) can be seen as a quadratic function of ρ_{ij} . Also, it is convex and its poles are located at $\rho_{ij} = 0$ and $\rho_{ij} = -\frac{2\bar{R}(t)}{\bar{A}} \leq 0$. Thus, C_6 monotonically increases with ρ_{ij} . As a result, j^* is the neighbor j with the smallest ρ_{ij} value. ■

Above theorem implies that it is optimal to choose the next destination target only based on the (shortest) travel time. This is clearly unfavorable as an agent could converge to oscillate between two targets in the target topology while ignoring others. Hence the importance of the denominator w term included in the RHCP objective function definition (13) is evident.

REFERENCES

- [1] J. Trevathan and R. Johnstone, “Smart Environmental Monitoring and Assessment Technologies (SEMAT) A New Paradigm for Low-Cost, Remote Aquatic Environmental Monitoring,” *Sensors (Switzerland)*, vol. 18, no. 7, 2018.
- [2] K. Leahy, D. Zhou, C. I. Vasile, K. Oikonomopoulos, M. Schwager, and C. Belta, “Persistent Surveillance for Unmanned Aerial Vehicles Subject to Charging and Temporal Logic Constraints,” *Autonomous Robots*, vol. 40, no. 8, pp. 1363–1378, 2016.
- [3] X. Meng, A. Houshmand, and C. G. Cassandras, “Multi-Agent Coverage Control with Energy Depletion and Repletion,” in *Proc. of 58th IEEE Conf. on Decision and Control*, 2019, pp. 2101–2106.
- [4] S. L. Smith, M. Schwager, and D. Rus, “Persistent Monitoring of Changing Environments Using a Robot with Limited Range Sensing,” in *Proc. of IEEE Intl. Conf. on Robotics and Automation*, 2011, pp. 5448–5455.
- [5] N. Zhou, C. G. Cassandras, X. Yu, and S. B. Andersson, “Optimal Threshold-Based Distributed Control Policies for Persistent Monitoring on Graphs,” in *Proc. of American Control Conf.*, 2019, pp. 2030–2035.
- [6] S. Welikala and C. G. Cassandras, “Asymptotic Analysis for Greedy Initialization of Threshold-Based Distributed Optimization of Persistent Monitoring on Graphs,” in *Proc. of 21st IFAC World Congress (to appear)*, 2020.
- [7] N. Zhou, X. Yu, S. B. Andersson, and C. G. Cassandras, “Optimal Event-Driven Multi-Agent Persistent Monitoring of a Finite Set of Data Sources,” *IEEE Trans. on Automatic Control*, vol. 63, no. 12, pp. 4204–4217, 2018.
- [8] X. Lin and C. G. Cassandras, “An Optimal Control Approach to The Multi-Agent Persistent Monitoring Problem in Two-Dimensional Spaces,” *IEEE Trans. on Automatic Control*, vol. 60, no. 6, pp. 1659–1664, 2015.
- [9] Y. Khazaeni and C. G. Cassandras, “Event-Driven Cooperative Receding Horizon Control for Multi-Agent Systems in Uncertain Environments,” *IEEE Trans. on Control of Network Systems*, vol. 5, no. 1, pp. 409–422, 2018.
- [10] C. G. Cassandras, Y. Wardi, C. G. Panayiotou, and C. Yao, “Perturbation Analysis and Optimization of Stochastic Hybrid Systems,” *European Journal of Control*, vol. 16, no. 6, pp. 642–661, 2010.
- [11] W. Li and C. G. Cassandras, “A Cooperative Receding Horizon Controller for Multi-Vehicle Uncertain Environments,” *IEEE Trans. on Automatic Control*, vol. 51, no. 2, pp. 242–257, 2006.
- [12] Y. Khazaeni and C. G. Cassandras, “Event-Driven Trajectory Optimization for Data Harvesting in Multi-Agent Systems,” *IEEE Trans. on Control of Network Systems*, vol. 5, no. 3, pp. 1335–1348, 2018.
- [13] R. Chen and C. G. Cassandras, “Optimization of Ride Sharing Systems Using Event-driven Receding Horizon Control,” in *Proc. of 2020 Intl. Workshop on Discrete Event Systems (to appear)*, 2020.
- [14] S. C. Pinto, S. B. Andersson, J. M. Hendrickx, and Christos G. Cassandras, “Multi-Agent Infinite Horizon Persistent Monitoring of Targets with Uncertain States in Multi-Dimensional Environments,” in *Proc. of 21st IFAC World Congress (to appear)*, 2020.
- [15] D. P. Bertsekas, *Nonlinear Programming*. Athena Scientific, 2016.
- [16] S. Rosenberg, “Conics.” [Online]. Available: <http://math.bu.edu/people/sr/GandS/handouts/Chapter6.pdf>
- [17] D. Auckly, “Solving the quartic with a pencil,” *American Mathematical Monthly*, vol. 114, no. 1, pp. 29–39, 2007.